Exploring neural model for path integration on a bio-mimetic robot

Danilo Orlando

Master of Science
Artificial Intelligence
School of Informatics
University of Edinburgh
2012

Abstract

Acknowledgements

I would like to thank my supervisor, Barbara Webb, for his insight and his support. I would also like to thank Michael Mangmann for the initial explanations and insight on his work on ants.

Declaration

I declare that this thesis was composed by myself, that the work contained herein is my own except where explicitly stated otherwise in the text, and that this work has not been submitted for any other degree or professional qualification except as specified.

(*Danilo Orlando*)

This is dedicated to you, the reader.

Table of Contents

List of Figures

Chapter 1

Introduction

Path Integration (PI) refers to the ability of summing small path increments along a trajectory in order to calculate the final position with respect to the initial position.

The term , conied by Mittelstaedt [**?**], indicates a form of dead reckoning first postulated by Darwin [**?**, **?**] in 1873, to describe a proprioceptive system of navigation in invertebrates. To accomplish this task a compass for retrieving heading position (with respect to a reference point) and a way to compute distances are needed, together with the cabability of storing and representing these information. Path integration is an important navigational strategy observed in many species such spiders , crustaceans , insects , birds and mammals [**?**, **?**].

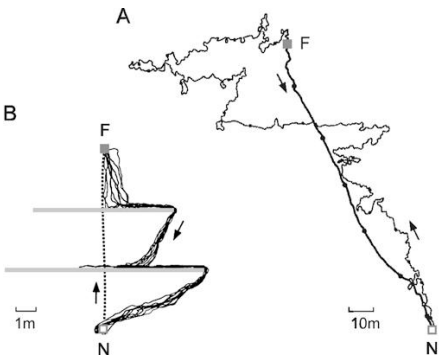

Figure 1.1: Example of Path integration in a desert ant. A After a tortuous foraging excursion the ant returns home in a straight path. B In the presence of obstacles .From Wehner [**?**]

An outstanding example of path integration can be found in the desert ant Cataglyphis [**?**, **?**]. After long tortuous outbound excursions for foraging , this insect can return to its home position exhibiting a straight path trajectory , updating the homing vector correctly in the presence of obstacles. This behaviour, which intrigued Pierotz and Cornetz [**?**] in the early 1900s has been object of studies for decades.

Different animals employ different information and representations, based among other factors, on their sensory system,leading to possible different mechanics and different scenarios in the way

path integration is implemented in a system.

In mammals and expecially rodents [**?**] Head Direction and Place cells in the hyppocampus [**?**, **?**, **?**] are used to combine a vector representation of the input provided by the sensory system, into a topographic , cartesian map represented by a population code of neurons responding to particular preferred direction.

In insect two essential components for the navigational system are a polarization compass and an internal odometer cite [**?**].

The compass is derived by analyzing the peculiarities of the pattern of polarization of the sky, combined with a spectral analysis of the skylight distribution.This mechanism ,involving specialized photoreceptors in the compound eye of the insect and specific neural pathways that process the sensory signal, is a common characteristic of many different species, in particular the Orthoptera (e.g. [**?**, **?**]) and Hymenoptera (e.g. [**?**, **?**, **?**]).

Polrasitation vision represent is one of the most important pre-requisites for navigation in insects and , together with a mean of measuring distances form the basis for vector navigation.

1.1 Motivation

The scope of this work is to explore possible neural dynamics and mechanism involved in processing skylight polarization patterns and implement a model ,based on biological foundings , to derive heading information from the sensory system in an insect. By trying to emulate neurological data and integrate it with pre-existing functional models of path integration,the project aims to provide a base for the understanding of how path integration can be implemented by a combination of specific neural circuits and how these principles can used to develop a biomimetic robot inspired by the navigational strategies found in insects.

Insects are able to exhibit complex mechanisms of navigation , in many ways similar to the one found in vertebrates, and ,having a smaller and relatively simpler brain are more easy to study from a neurobiological point of view in respect to more complex neural apparatus found in mammalians.

Idiotetic cues and in particular compass and odometer are two fundamental components in robotics and path integration, which rely on them , is a problem that has fascinated for years generations of biologist and scientists. In robotics, an outstanding example of the importance of path integration is the NASA's

Mars Rover employed in the Pathfinder mission [**?**].

There exists a variety of Path Integration models in literature [**?**, **?**, **?**, **?**] inspired by biological evidence (e.g [**?**,**?**,**?**,**?**,**?**],Wessnitzer2008, Wehner1989,Wittmann1995). Few models hovewer are able to incorporate more recent neural data and use realistic or simulated sensors which provide an input similar to the one processed by brain of insects. Furthermore , except for model based on mammalian brain, no model make use of more biologically plausible spiking neurons in path integration systems.

The project hence has the double role of exploring possible scenarios for the implementation of more realistic neuroarchitecture for controlling biomimetic robots and secondarely anlyses some data on real neural systems and test some of the possible ways in which these foundings can be combined to form a complete circuit for polarotactic navigation and path integration. In this second regard a complete simulation of the known pathways involved in polarized light analysis could be used as a mean to develop new experiments and test some hypothesis which are difficult to explore in a laboratory environments [**?**]. As an example electrophysiological recording under real sky conditions are difficult to set up and a computer simulation could provide some useful insights.

The project is far from being complete and exhaustive , but it constitute a starting point for further developments in the pursuit to the realization of these two big objectives.

1.2 Objectives

The main objectives of the project were:

- Explore the neural dynamics of polarotaxis in insects
- Provide a spiking neural networks based on realistic biological foundings
- Explore possible dynamics for path integration
- Explore problematics concerning robot implementation

The problem of deriving a complete system for path integration based on realistic neural dynamics can be decomposed in the following steps:

1. Provide a modelling of polarized light sensing

2. Model neural dynamics of polarization vision in insects
3. Formulate an hypothesis on the different role of the different area and the relative computation performed
4. Discuss dynamics for spatial informations storage in the brain of an insect
5. Discuss a mechanism for sensorimotor control driven by polarization vision

Each of this steps require a consistent amount of work if there is the desire to match the physiological data, expecially considering that this data are relative to different species and the exact topology and signal information processing performed by the brain for polarized vision and path integration are not known.

Every single step necessary to solve the task is a non trivial problem in literature and in some cases, when it comes to biological realism, only some possible insights are available. As a complication there was no proper dataset to analyze for possible data mining analysis.

Hence,as we will see , it was not possible to solve all the problems and provide a detailed implementation for each of the objective, and for some cases some ideas for possible realizations are provided. In particular most of the work has been devoted to the early stage of processing of polarisation light, as this crucial aspect is absent from the majority of pre-existing models. It was also not possible to test and implement the model on a real robot due to the unrelaibility of the available sensors and delays in the realization of possible implementations of the simulated circuits based on neurological foundings. To account for the lack of sensors a computer simulation of polarized skylight distribution has been developed and the project changed its original focus.

1.3 Outline

In the next section a review of some of the most important result from electrophysiological recordings on real insect is proposed.As we will see a dedicated network of neurons from various area of the brain of an arthropod are dedicated or sensitive to polarisated ligh and details about specific pathways of this complex signal processing apparatus start to emerge.**Chapter 3** review some of the exsisting models for path integration, completing the picture of the essential elements on which the project is based. **Chapter 4** describes the implementation

of the Rayleigh Sky model for simulating real pattern of polarization in the sky and some of the problematics which lead to a switch in the original focus of the project, in particular the implementation on a real robot. In **Chapter 5** the simulation of photoreceptors and Pol-Neurons are described, together with the results of these analysis. In **Chapter 6** we found the results of experimenting with the existing model of Sakura et. al [**?**] and the development of a version based on biologically plausible spiking neurons. **Chapter 7** reports the design for a possible complete architecture for polarization compass and path integration and a plan for the implementation of the newtork on a real robot. Finally **Chapter 8** discusses the whole work and possibilities of development for further work.

Chapter 2

Background

This chapter present an overview of part of the most relevant literature about the biological foundations of path integration and in particular of the polarization vision in insects, which is an essential prerequisite for the implementation of path integration in arthropods. Different species have inevitably different characteristics and it's difficult to integrate all the informations from such a varierity of animals, but we can define four essential components of a system implementing path integration:

Orientation system: Path integration requires at least a mean to compute the actual bearing angle with respect to some reference point and coordinate system and a way to compute distances. Many species and especially insects [**?**] rely on allothetic optical cues such as the sky position, the distribution of polarized light in the sky or the spectral distribution of the skylight in order to derive a compass system which is usually more reliable than a proprioceptive system. Generally landmark navigation and vision are considered as complementary but not essential components of the PI system.

Odometer: In absence of allothetic cues for orientation and for computing distances an agent rely on idiothetic signals. The way distances are computed in insects for path integration is still one of the most unsolved issues [**?**], altough Ronacher and Whener [**?**] propose self induced optic flow as an internal odometer. Another possible cues for measuring travelled distance is step counting based on mechanoreceptor signals.

Internal Representation: The way sensory signal are processed and represented internally by the animal is still a mistery. Wheter there is a popu-

lation code encoding vectors or phase-amplitude components of the signal and the way all this informations are encoded and converted to azimuthal representation is still unknown. Different hypothesis exist and are examined in the following sections, but which kind of cognitive maps are involved in the path integraton system is an open question.

Memory System: The continuous integration of single path increments and the way they are stored is directly connected to the problem of defining the specific representation used by the PI apparatus. It could be that some of all or the single waypoints along an excursion are stored and integrated or only a few or the last vector is hold in memory. In any case a system for storage of the information and integration with other cues such as landmarks is necessary for a complete navigational system.

2.1 The polarization compass

Arago in 1809 was the first one to point that , as a result of scattering phenomena in the atmosphere, the light from the sun is partially linearly polarized in 1871 [**?**, **?**]; as a consequence at any point in the celestial hemisphere there is a predominant orientation of the electric field (e-vector) and a specific degree of polarization. Depending on the position of the sun in relation to an observer at a specific altitude and longitude, polarization of the skylight follows a specific distribution which is arrangend in concentric circle around the sun (Figure 2.1).

A lot of different species such as crickets,ants, locusts and bees [**?**] ,among others, have been found capable of exploitong these patterns of polarization and use them as one of the main navigational cues. The significance of polarized light for path integration is such that the *Cataglyphis* for instance, when trained only with a portion of the polarization pattern and than tested under the full polarization patterns , exhibit systematic error which are not present if trained with the whole pattern. So even if the ant in sensitive to the spectral distribution of radiance, its main orientation cue remain the polarized light, even in non optimal condition [**?**, **?**].

A fundamental question in polarization vision is, how the insect can exploit the pattern of polarization and derive accurate compass information? In principle the problem can be resolved using trigonometry. Since the e-vector is always

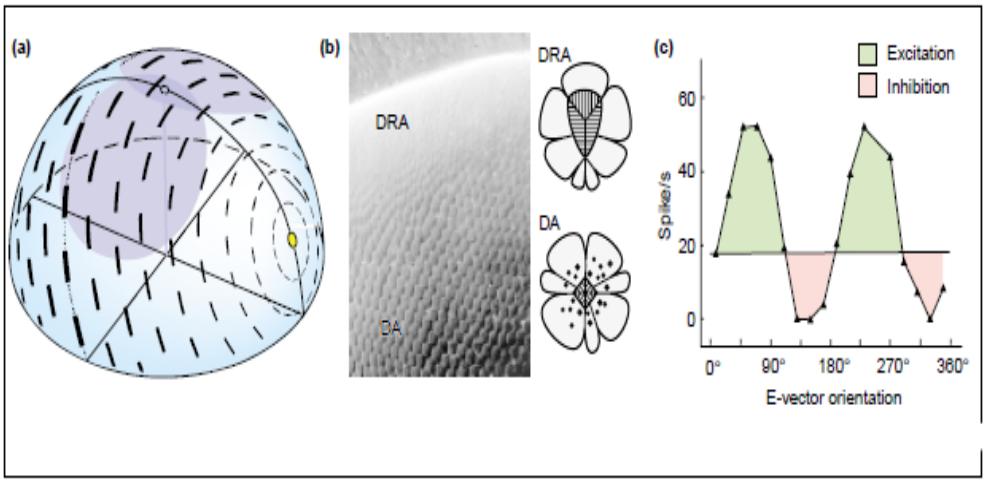

Figure 2.1: Polarization vision fundamental.(a) Schematic diagram of celestial polarization pattern around the sun (yellow circle). The bars indicate the angle of polarization and their width the degree of polarization. (b)Specialized ommatidia of the DRA compared to regular ommatidia (DA) in a field cricket, with a schematic diagram of the microvilli arrangememnt.(c) Example of the response of a POL-neuron to different e-vectors orientation.Green:excitation,Red:inhibition.From [**?**]

perpendicular to the plane of polarization ,by measuring two points and running two semicircles on the celestial emisphere at right solid angles from the local direction of polarization , the sun position is determined by the point at which this circles intersect. The position is not unambiguous as there are two such points, in the solar and antisolar half of the sky.The solar merdian however can be determined by a spectral analysis due to the different radiance distribution [**?**, **?**]. But we still don't know if the insect has the ability of doing such complex computations and moreover it is able to orient even observing a single patch of the sky ,without the need to observing two points. So where this outstanding ability come from? The answer is not yet know , but a specific set of neuropils and specialized polarised light analyser have been found in different arthropods. Starting from specialized photoreceptors in the Dorsal Rim Area (DRA) of the compound eye of an insect, a set of dedicated neurons responds tonically to specific e-vector orientations and the information flow through the central body following specific pathways.

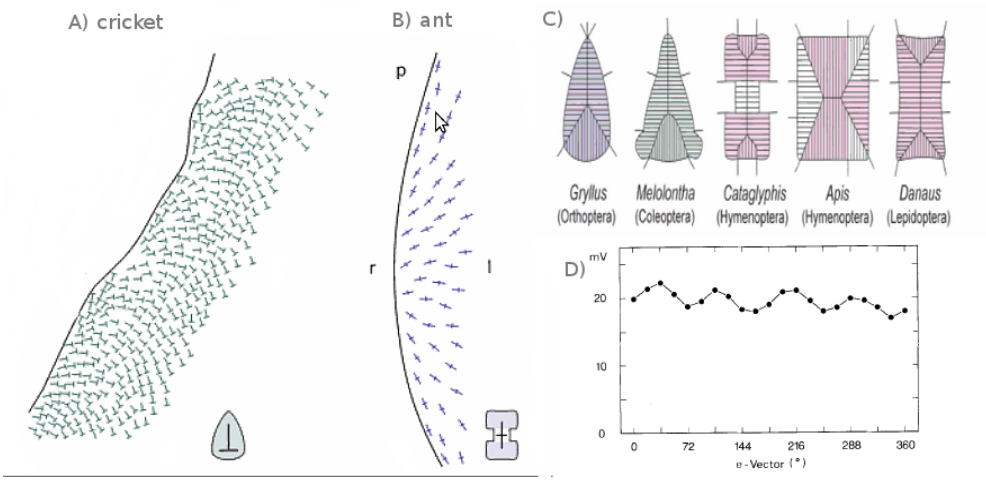

Figure 2.2: Photoreceptors in the DRA.(a) Arrangement of ommatidia in the cricket. (b)Arrangement of ommatidia in the desert ant.(c) Schematic cross-section of microvilli arrangement in different species d) Voltage recording from a UV-cell in the DRA of a desert ant. a,b,c adapted from [**?**]. d) adapted from [**?**]

2.1.1 Photoreceptors

A small area in the lateral part of the compound eye of insect, known as DRA, contains a set of photoreceptors which reported in a series of electrophysiological recording a high sensitivity to the light in the blue or UV spectrum, differently from the rest of the dorsal area DA. In the apposite compound eye of arthropods the photoreceptors are elongated cell (ommatidium) contained in the retina. Each ommatidia contains a set of fused rabdhomere, which carry the photopigment in tubular protuberances called microvilli [**?**]. A degraded optic make the visual field of the ommatidia in the DRA wider than the other part of the eye and suitable for scattering phenomena. Moreover the particular orthogonally orientation of the microvilli make this photoreceptors particularly sensitive to polarized light and each set of microvilli constitute a pair of antaghonist sensors with a sinusoidal response to different e-vectors orientation [**?**, **?**] and a preferred orientation which depends on the optical axis of the analyzer with respect to the animal orientation. The cell indeed responds maximally when the e-vector is oriented parallel to the rhodosphine molecule carried in the microvilli [**?**, **?**].

The distributions of preferred orientations, the width of the visual field and the arrangment of the ommatidia along the DRA vary across the species (figure 2.2). In crickets for example the ommatidia are arranged in a circular pattern , while in ants exhibit a characteristic fan shape across each of the contralateral

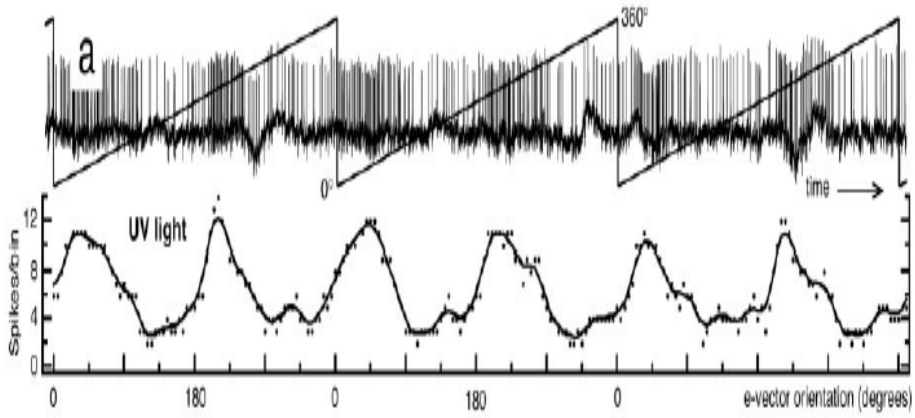

Figure 2.3: Pol-neuron response.An example of voltage trace (upper row) and average firing rate(lower row) of a pol-neuron in the optic lobe of a desert ant in response to a continuous rotating e-vector.From [**?**]

section of the longitudinal axes with respect to the head of the insect. The field of view is wider in crickets , reaching up to 20 ° [**?**] , due to the major optic degradation, while in ants is about 5 ° [**?**]. As a result spatial integration is performed in the DRA of crickets,with a large area of the sky pooled on both emispheres. Each ommatidia point upward to a specific portion of the celestial emisphere, above the head of the animal. Hence each of the photoreceptors is a sampling station providing information about the evector distribution and degree of polarization to the rest of the brain.

2.1.2 Pol-Neurons

Polarization sensitive neurons (pol-neurons) receiving input from a set of ommatidia with orthogonalli oriented microvilli have been found in the optic lobe of desert ant [**?**], in the lamina and medulla of the desert locust [**?**], in the optic lobe of the cricket [**?**].

In all cases this neurons, which show similar morphological characteristics, when stimulated with artificial polarizer and different e-vectors orientation ,responded with an alternating part of inhibition and excitation, with respect to a background activity which vary among the different species, with minimum and maximum activity occurring at a period of 90 °. The point of maximum activity defines the preferred orientation of the pol-neuron.

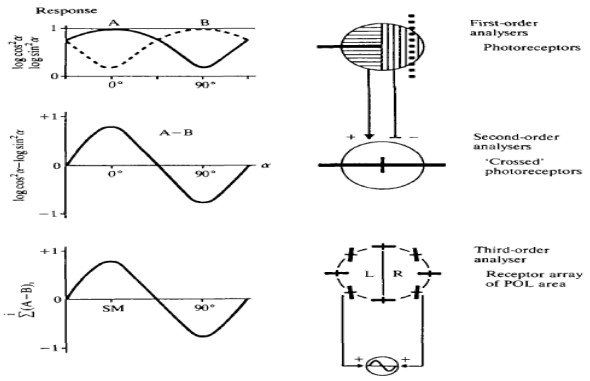

Figure 2.4: Hypothetical schema of three polarization analysers.The signal of the photoreceptors(top row) is passed to a pol-neuron (centre) which compute the difference of the two antagonistic sinusoids. The differences are than integrated in the optic lobe (bottom row).From [**?**]

Together pol-neurons and ommatidia in the DRA costitute the first stage in the construction of the polarization compass. Whener [**?**] defined the ensamble of photoreceptors and polarization sensitive neurons 'matched filter', referring to a set of spefific sensors developed to solve a speficic task, without the necessary presence of a centralized system of information processing or the notion of cognition.The author hypothized a three stage process. At the first stage the signal of two mutually ortogonally oriented microvilli is sent to a pol-neuron.The neuron computes the log differences of these two sinusoids and finally the signal coming from different analyzer is averaged during the third stage of processing. This simple schema illustrate the combination of a process of optical and neural integration in the optic lobe. In crickets for example each pol neuron receive input from about one third of the ommatidia (200) in the ipsilateral emisphere. As a result the field of view of a pol-neuron is enlarged and measures the polarization patterns in a relatively big portion of the sky. Based on the alignment of the optical axes of the photoreceptors and on the combination of the input in the pol-neurons different distributions of preferred orientations arise in the optic lobe.

In crickets the e-vector eliciting the maximal responses are clustered around three values (10 °, 70°, 130 °)at a distance of 60 °. In ants and locusts instead there are no predefinite classes of preferred orientations. The reson behind this differences and the absence of specific classes of preferred distribution in some species remains unclear, and pose a question about the validity of the hypothe-

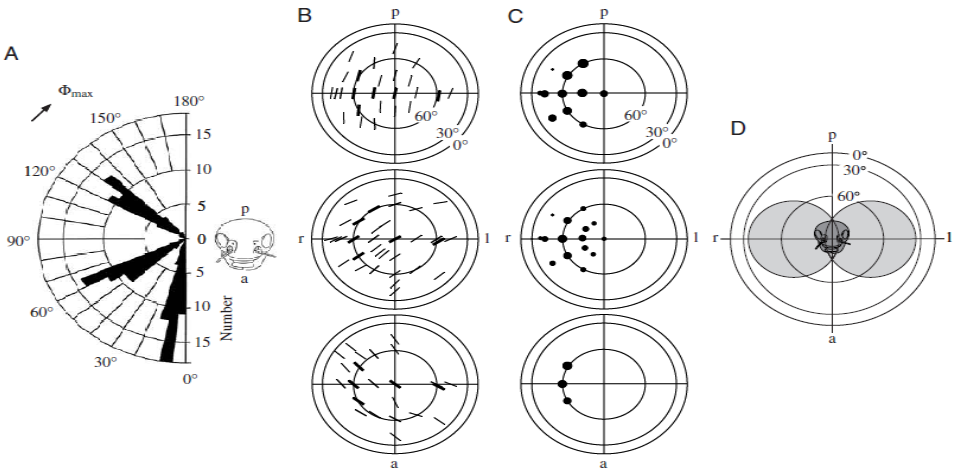

Figure 2.5: Neural integration in crickets.A) Distribution of preferred orientations in the POL1 area of crickets.The length of the bar indicate the number of neurons for each e-vector direction.B-D)Map of the data as zenith (center of the graph) projection of the upper hemisphere.Concentric circles represent different elevations. B)Distribution of preferred orientation in relation to the patch of the sky for three classes. Parallel orientation correspond to similar preferred orientation.C)Different sensitivity level (width of filled circles) in relation to the mapped position on the celestial emisphere. D) Width of the visual field of a pol-neuron (width of gray circles) as a result of neural integration. Map in polar coordinates.From [**?**]

sis of the triplept code developed by [**?**]. Kirschfeld proposed that to determine unambiguously three e-vectors at least three sensors with different oriented optical axes and pointing to the same part of the sky are necessary. Buy successive measurement and comparison noise informations such as degree of polarisation and spectral intensity can be removed and the single e-vector can be derived. Altough it is not tought that insects rely on single e-vectors detection, due to spatial integration and wide field of view, the 'successive method' or 'instantaneous detection' method [**?**] of Kirshfeld could be in principle applied by pooling the signal from at least three different large integrators and ,by antagonistic comparison, derive the azimuthal angle with respect to the sun through a series of 'compass neurons' hypothetized by different authors [**?**, **?**, **?**] and similar to the head direction cells found in rats. Such a method , as we will se in the next chapter has been successfull applied in simulated models as the network of Sakura [**?**] and the Sabahot robot of Lambrinos []. The distribution of preferred orientations in ants and bees , the reason and role of binocular input and the way informations from POL

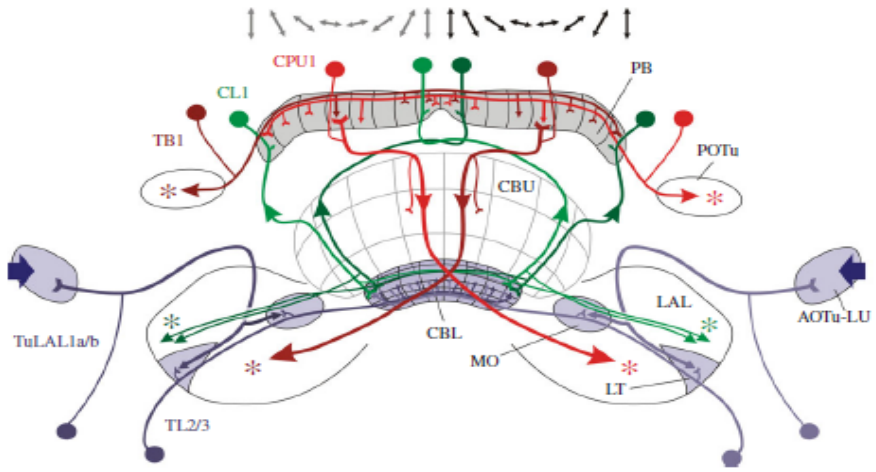

Figure 2.6: Polarization vision network.Hypothized pathways in the brain of the locust. Blu lines represent the input stage from the optic lobe, green arrows the input to the central complex from TL neurons to the CL neurons and in the PB. Red arrows are the output of the central complex, to the lateral triangle. From [?]

neurons is transferred to hypothetical compass neurons nowever is not clear, as well how exactly the comparison among different patches is accomplished. What is clear is that by neural and spatial integration pol neurons help to improve the accuracy of the e-vector detection under not optimal conditions, such as cloudy sky, when the degree of polarization is reduced and it's proximal to the sensitivity threshold of the single photoreceptors. In this way the animals are still able to orient themselves even if a small portion of the sky is visible [?, ?, ?, ?].

2.1.3 The central complex of the locust

A complication in the disentaglement of the neural dynamics of polarized light vision and path integration comes from the variety of the experiments on an etherogeneous set of species. The majority of behavioural experiments are on honeybee and ants , while electrophysiological recordings exist mainly for POL1 neurons in crickets and neurons of the brain of the desert locusts [?]. From different studies (e.g [?, ?, ?]) a specific schema emerge which brings the polarization signal from the DRA and the optic lobe to the anterior optic tubercle, and from here, through a series of neurons with specific morphological characteristics into the central-complex of the brain of the insect. The central complex [?] is a group of neuropils in the centre of the locust brain , divided in three major sections: the

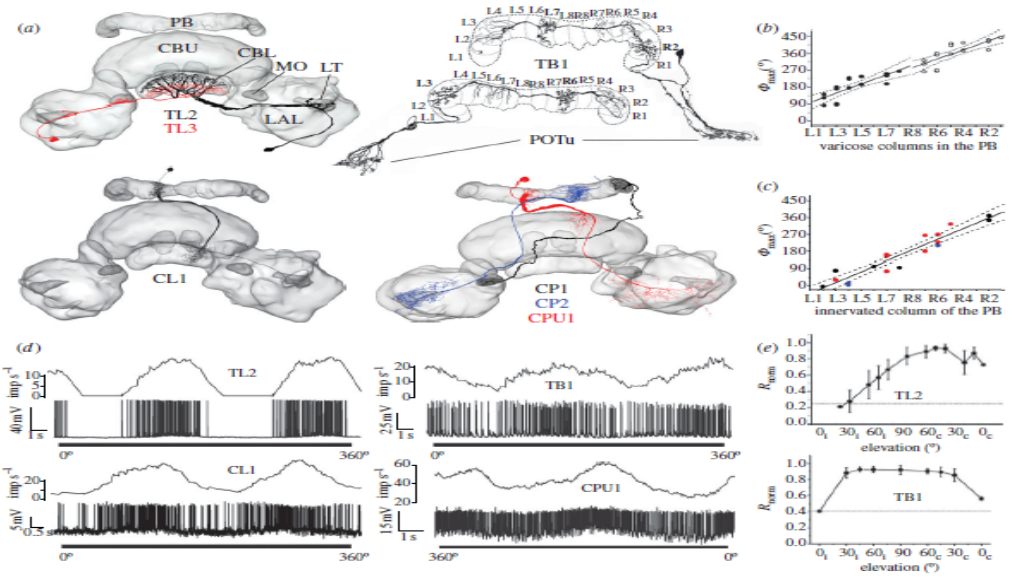

Figure 2.7: Recordings from central complex neurons.Different recording from different types of polarization sensitive neurons in the brain of the locust.a)3-d mapping of the position of the neurons in the brain.b)Preferred orientation regression analysis of TB neurons, in relation to the specific column (x axis) to which they project in the PB. Columns are named from 1 to 8, with L indicating the left emisphere and R the right one. c)Same plot for the CP neurons.d)Example voltage traces and mean response of different kind of neurons to a rotating polarizer.e) Mean receptive field for TL2 and TB1 neurons for different elevation of the stimulus. From [**?**]

lower and upper division of the central body (CBU and CBL) and the protecerebrum bridge (PB). The architecture of the central complex consist of a series of 16 vertical columns, 8 for each emisphere and of multiple horizontal layers in the CBU and CBL. A series of tangential and columnar neurons interconnect specific columns among the section of the central-complex or bring input from early stage of processing or send the output of the processing unit to the lateral triangle (LAL), the median olive (MO) and the toracic ganglia, with some neurons carrying feedback signals to other sections of the brain (figure 2.6). The set of neurons tought to be most relevantly for polarization vision are the tangential neurons (TL) in the anterior optic tubercle, the CL neurons in the CBL, the tangential neurons (TB) in the PB and the CP and CPU system of the upper division of the central body CBU. All these neurons exhibited strong sinusoidal response when stimulated with a rotating polarized light , altough different peculiarities characterize their response [**?**, **?**, **?**]. After polarization sensitive enhancement in the

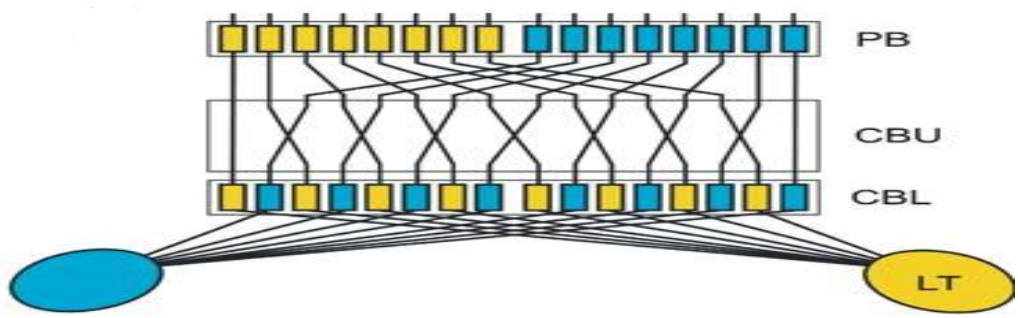

Figure 2.8: Example of columanr arrangement in the central complex. Each column of the CBL project to specific columns in the PB, following a predefinite scheme. Adapted from [**?**]

optic lobe, spectral cues are integrated in the tangential neurons (TL) , receiving input from the Lotu and Tutu neurons in the anterior optic tubercle. These neurons indeed are sensitive also to unpolarized light and may used to signal the position of the sun by analyzing the spectral distribution of the intensity of the light, which vary in relation to the wavelenght. In this way is it possible to disambiguate if the animal is facing the solar or antisolar meridian portion of the skylight.

TL neurons2 [**?**] integrate the signal of ipsi and contralateral eye, while TL3 neurons receive input almost esclusively by the ipsilateral eye. Both classes project to specific layers of the lower division of the central body and are thought to be the input stage of the contral complex machinery, having also the role of transforming the input from eccentric to more zenith centred. From here the signal is analyzed by the CL neurons in the CBL. CL neurons reported [**?**] the narrower tuning width of all the neurons in the central-complex and a relative high signal-to-noise ratio.If we add to this the columnar arrangement, CL neurons are the main canditate for representing the compass neurons discussed above. Cl neurons project to specific columns in the PB through TB neurons and from this the signal reach the the upper division of the central body and reach, by intermediation of the CPU1 system the motor neurons in the lateral triangle. The particular arrangement of neurons in the PB and CBU (figure 2.8) make think that the insect hold a map of the e-vector distribution, maybe in the form of a population code. Morover the CBU is responsible for other visual tasks and motor control. Indeed TB and CPU neurons have wider field of view and lower

signal to noise ratio with respect to TL and CL neurons, suggesting that their higher background activity carry signal from other neural machineries.

The PB-CBU loop could hence be responsible of performing path integration and implementing other navigational strategies.

2.2 Summary

This chapter presents a concise overview of the most relevant biological founding about polarization vision in arthropods, which is a pre-requisite for path integration and the main focus of this work.

Thruogh a specific network of specialized interneurons, polarization signals are driven from the optic lobe to the central-complex and here probably integrated with other spatial information. The specific arrangement of columns in the central body of the insect make think that arthropods could hold a cognitive map of the e-vector distribution from the polarized light and use it to derive a compass, maybe using a population code and compass neurons similar to the head direction cells of rats.

Unfortunately little is known about the specific informations hold by the different areas involved in polarotactic vision and on the specific computations performed by single neurons and group of neurons [**?**, **?**].

For example is not known if a unique single map of e-vector distribution is mantainend by the insect or if multiples complimentary map occurs together and where and how they are compared. Another open question is how the e-vector information is converted to azimuthal direction, or alternatively in relatively subsequential change of directions, within a specific system of coordinates and how this information is stored to perform successive computation. The role of binocular input is also another controversial point.

Some models discussed in the next chapter forms hypothesis on how this tasks could be performed, but their specific implementation in the brain of arthropods has to be confirmed.

Chapter 3

Models for path integration

This chapter offers an overview on some of the theoretical and computational models which attempted to provide a qualitative or quantitative description of path integration. In particular the focus will be on the network of Sakura et al and Wessnitzer et al, as can be easily integrated in the model of the sensory periphery developed during the project.For reasons of space many models are just briefly cited. Two great and more exhaustive review can be found in [**?**] and [**?**].

3.0.1 Mathematical Models

Formally the problem of path integration can be formalized as follows:

Given a start position X, an agent performing path integration must mantain its current position with respect to X by subsequent integrations of its movement vector. In this way if P is the current position an agent can return home simply following G=-P [].

To estimate its current position the agent must rely on a mixture of allothetic cues, such as a sun compass or a polarization compass and idhiotetic cues, such an internal odometer to measure distances.

Jander [] was the first one that tried in 1957 to define mathematically the problem, proposing a mechanism of continuous integration of the angle with respect to a light source or a landmark as a mean of estimating the current position, assuming a constant speed. Since than a variety of mathematical models have been devoted to describe path integration, based on geocentric [] or egocentric [] systems either in polar [] or cartesian coordinates []. In the bicomponent model of Mittelastaed [] each direction is scomposed in its sin and cosine components with respect to an earthbound cartesian system of coordinates and the signals

from allothetic and idiotetic cues are merged by averaging the single components weighted by the distance traversed. The resulting coordinates (x,y) are then computed by trigonometry. The model provides a general correct solution of path integration, but is not based on experimental evidence on animals, and is not able to explain the occurrence of systematic error. Benhamou, Sauve and Bovet [] developed a similar trigonometric model but adding noise,using an animal centered coordynate system and attempted to provide a systematic study of the error in the system, trying to understand what is not influenced by random noise, differently from Mittelastaed which attributed the errors to a noise immanent to the computational process. In their reasearch they founded that greatest error is due to misestimation of idiothetic cues, while allothetic cues have less impact on the system,being negative correlated among successive estimation. Muller and Wehner [] (see also Hartmann and Wehener [], Whener and Whener [])criticized the approach of Mittelastaed of vector representation , as the overload due to the possible vector representation could be, in their opinion, not the solution adopted by the biological organism, despite the theoretical correctness of the model. They recovered the arithmetic approach of Janden (which is trigonometrically incorrect) assuming that the agent continuously record the distance travelled at each path increment s_n and the angular displacement from s_{n-1} The model of Muller and Wehner is a recursive and iterative process in which, at each step, given the angle $\theta with respect to the initial position, the animal, measures the current position \theta + \delta$,and compute the angular average weighted by the distance travelled. The animal hence store a polar vector (r_n, v_n), where $r_n = \int \cos(\theta - v) ds$ and $v_n = \int \frac{\sin(\theta - v)}{r} ds$. Muller and Whener were the fist able to successfully fit the data on ant 's beahviour [], at least for outbound journeys composed of two or three piecwise increments. However, as pointed out by Marjdssa [] , the model was unsuccessful in capturing other behavioural experiments as looped journeys and to predict, at each increment of a discretized path, each single position. More recently Merkle et al [] returned to a egocentric representation, but using Cartesia coordinates. The system of reference is constituted by the main body axes and each point, such as the nest, can be measured with respect to this system of coordinates storing a position vector G=(X,Y). The authors develop a two dimensial differential equation system in which $\frac{dX}{dt} = -v + \omega Y$ and $\frac{dY}{dt} = -\omega X$, where v is the forward speed and $\omega the angular turning rate. Such model is simple and doesn't require trigonometrical function. It is h$ 1001[]$suggests that such functions could be approximate employing piecewise linear or polynomia$

1001[], *butrequirestheimplementationofmultiplicationinaneuralcircuit.Maass*, *oneofthepion*
1001[?]*thatispossibletobuildneuralmodelsthatperformsaddiction*, *subtraction*, *comparisonand*

A network of this type however can have a large complexity, depending on the type of representations holded and it remains to see if this is compatible with the brain architecture of an insect and the specific dynamics of the neurons that built this machinery. There is some evidence [**?**] that multiplication can be implemented by specific neurons in the visual system of a locust and Nezis et Van Rossum [**?**] showed a mechanism form implementing multiplication based on firing rates, but if this is compatible with mathematical models of path integration remains an open question, as well as the biophysical significance of multiplication.

Moreover all these models are a temptative explanation of describing the behavioural foundings on different species of insects, but don't take into account how this computation is exactly performed and, most importantly, how the single cues are derived from the sensory system. In all this cases indeed, this crucial information is assumed as a given input to the model.

3.0.2 Biologically inspired Models

Motivated by the search for possible neural mechanism that implements path integration various neural netwroks model have been attempted during the years []. For example the network of Harthmann and Whener [] used a bicomponent model in which a linear chain of neuron encoded the distance travelled and a circular array was used as a population for encoding heading directions. Turetzky et al() proposed a population vector of neurons encoding the phase of Fourier components of the allothetic or idiothetic signal and each neuron represent the amplitude of a certain spectral component. Wittman and Sweghler [] uemployed the same strategy developing a bicomponent model in which one set of phasors encode for the heading direction and a second set of phasors for the homing vector.Both vectors are represented by the changing activity of a subpopulation of neurons. In this way the position can be updated relying only on vector arithmetic and the turning angle can be computed simply subtracting the current position from the homing vector.

Mittelastaed

Sakura

Wessnitzer

3.0.2.1 Sabahot

3.1 Summary

Chapter 4

Polarized light simulation

This chapter presents the results achieved and the methods adopted in the implementation of a system for simulating polarized light as an alternative to collect real sensor data. In the first section I discuss some of the problems with the available sensors, which lead to a switch on the project and required the construction of some synthetic data. I then present the Rayleigh sky model [**?**,]sed to simulate the distribution of pattern of polarized light and the input to the system. Finally, in section 3.2, the modelling of single photoreceptors and the construction of a model for the Dorsal Rim Area of an insect are reported.

4.1 Sensor problems

The original plan for the project was to study a possible spiking neural network implementation for polarotactic orientation and path integration on a real robot provided with polarized light sensors and test the architecture in a controlled environment in the lab.

The robot was a Kephera II Robot by K-Team coporation [**?**] provided with an extension turret which consent to add additional sensors to the default 8 infrared light sensors and an ambient light sensor. Using the turret a set of 8 photodiodes [detail, field of view] with a polarizer cap is mounted on the top of the robot as shown in figure... By rotating the polarizer cap is it possible to change the orientation of maximal response of the photodiode.

The arrangement of the sensors is such that photodiodes placed 180 °apart (with the axes S1-S5 in figure .. choosen as the body axis) correspond to a pair of orthogonally oriented photoreceptor and are theoretically able to simulate a the

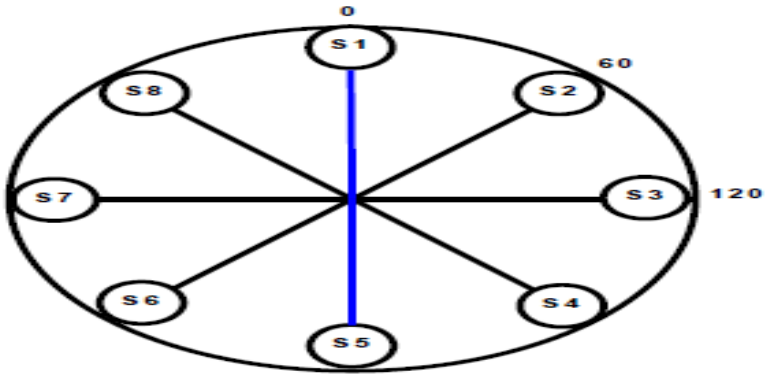

Figure 4.1: A schema of the photodiodes arrangement on the sensor board of the Kephera II robot.From [**?**]

antaghonistic signals provided by the ommatidia. Sensors labelled S1,S2 and S3 have the optical axis oriented at 0,60 and 120 degree with respect to the body axis and can be used to simulate the distribution of preferred orientation in crickets.

The lab environment is provided with a series of bulp fluorescent lamp generating a 100% degree of polarization (which is unrealistic under sky conditions).

insert picture of the robot and the arena

insert picture of the sensor board

The sensor board has been already extensively examinated by Hiremath and Mangann [**?**] during a previous MSc project and Hiremath found that the sensors were really noise , especially near the maximal response , and they suffered from motor interference and the noise of the ambient light. The author provided an heuristic correction to the response but the sensors were overall not usable.

There was at the beginning the perspective of receiving or develop modified improved sensor but also this road was abandoned. Since the main idea was to collect at first a series of data from the sensor board and develop a computer simulation, and since the main focus was to trying to match and explore the biological dynamics of polarataxis, we decided with the supervisor to implement a computer simulation of the skylight polarization and base the analysis on the simulated data. In this way we could avoid a priori sensor problems in the experiments which tried to match neurobiological data.

The research and implementation of a simulated environment with a sufficient degree of realism has been very time consuming and lead to a delay in the development of the subsequent parts of the project.

In contrast the creation of a virtual environment with more biological realistic

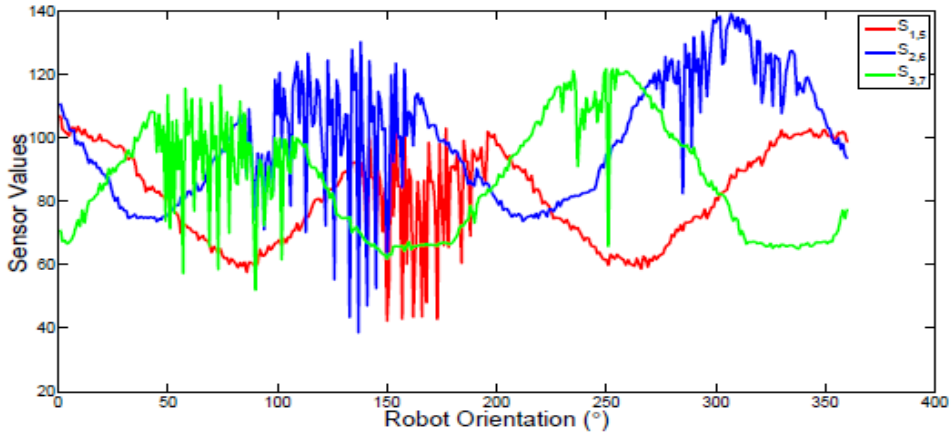

Figure 4.2: Example of the response of three pairs of antagonistic photodiodes on the Kephera II robot. Notice the very high level of noise in proximity of the maximal response. From [**?**]

input signals has opened the doors to a set of new interesting scenario for the exploration of the underlying mechanism of polarization orientation and path integration.

4.2 Rayleigh sky

As a resulting of the scattering phenomena in the atmosphere the electromagnetic wave reaching the earth from the sun is separated into two components perpendicular to each other.When the two components are in phase we speak of linear polarization, otherwise of circular or elliptical polarization. The state of polarization is described by a four-element vector introduced by Stokes (1852) (see [**?**] for a formal description) which are dependents by the degree of polarization , the angle of polarization (the angle of the direction of the oscillation with respect to a given plane) and the ellipticity of polarization.

The Rayleigh scattering is an approximation of the Mie's solution to the Maxwell's equations for scattering of an electromagnetic wave by a sphere and describes how particles in the atmhospere scatter the incident light for particles that are up to 10% smaller than the wavelength of the incident light [**?**]. Under the Rayleigh framework the skylight incident at any point observed on an ideal celestial emisphere (Poincare sphere) by an agent placed at the center of the sphere has well determined pattern of polarization and the degree of polarization and

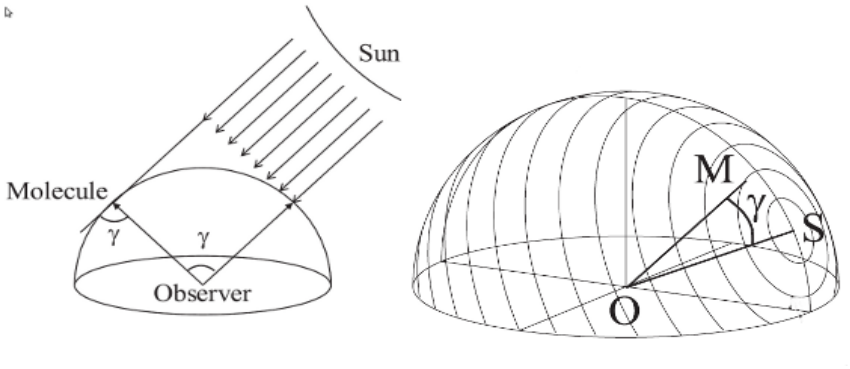

Figure 4.3: A schema of the arrangement of concentric circle in relation to the scattering angle γ.Adapted from [**?**]

intensity depends only on the scattering angle, while the angle of polarization (with reference to the local meridian) are arranged in concentric circle around the sun (see figure 4.4) . As a consequence of the ephemeris function of the sun the pattern of polarization change during the day and are also dependent on the location of the observed point. Since each point on the surface of the infinite Poincare sphere is equidistant from the observer the system can be described by a polar coordinate and zenith centred axes of coordinates in which each point $p(\theta, \phi)$ has an elevation θ and an azimuthal angle ϕ. We adopt the convention that angles are measured in a counter-clockwise manner, with the x axes correponding to the E-W axes and the y axis corresponding to the N-S axes. Note that usually, in literature, West and East point are inverted.The sunset hence will be at East , at the point (0°,0°) and the twilight at (0°,0°). Furthermore we adopt the convention to indicate with θ_s and ϕ_s the elevation and azimuth of the sun. The elevation ranges in [0°,90°], with 90°corresponding to the zenith and the azimuth in [0°,360°]. In this way is more convenient to visualize the pattern of polarizations and also to compute the polarization at each point.

Using the Rayleigh sky model the formula for computing the degree of polarization, intensity of the scattering light and the angle of polarization can be computed as (see [**?**] for the mathematical derivation):

$$\cos(\gamma) = \sin\theta_s \sin\theta \cos\psi + \cos\theta_s \cos\theta \tag{4.1}$$

$$d = \frac{\sin^2(\gamma)}{1 + \cos^2(\gamma)} \tag{4.2}$$

where γ is the scattering angle,$\theta_s$is the solar elevation, θ the elevation of the observed point and $\psi$the azimuthal distance of the observed point from the solar

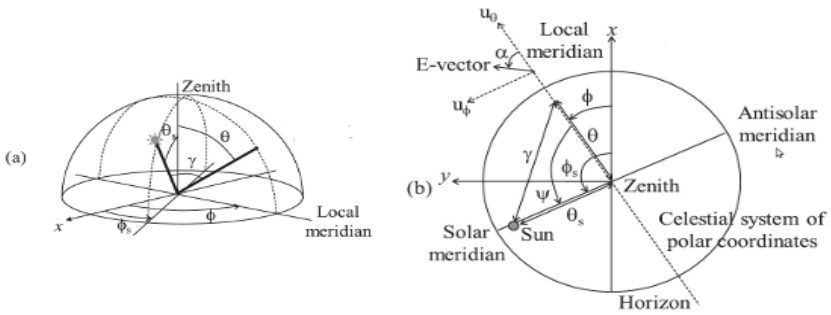

Figure 4.4: The celestial polar coordinate system in 3D (left) and 2D(right). Adapted from [**?**]

meridian as depicted in figure .The scattering angle varies between 0°for direct light and 90°for the farest points.

The intensity of the scattered light is :

$$I(\gamma) = \frac{K}{\lambda^4}(1 + \cos^2(\gamma)) \tag{4.3}$$

where λ is the wavelength. Here we used a value of λ =400nm, for the UV receptors.

K is a constant computed as:

$$K = a_p^2 I_0 \frac{16\pi^2}{r^2} \tag{4.4}$$

$$I_0 = E_0^2 \cos^2 \frac{2\pi ct}{\lambda} \tag{4.5}$$

where E_0 is the amplitude of the electric field, c the speed of light, t the time of optical integration and a a constant of polarization. The constant a was used to model the polarization sensitivity of the photoreceptors and determine their maximal response.

Finally the angle of polarization is computed from:

$$\tan(\alpha) = \frac{\sin\theta_s \cos\theta \cos\psi - \cos\theta_s \sin\theta}{\sin\theta \sin\theta_s \sin\psi} \tag{4.6}$$

Using these equations a tool (descriped in the Appendix) , which consent to change manually the location of the sun and create a map of the pattern of polarization, using a sampling of the infinite points on a sphere. The program serves also as the basis, how we will see in the next section, for observe how a

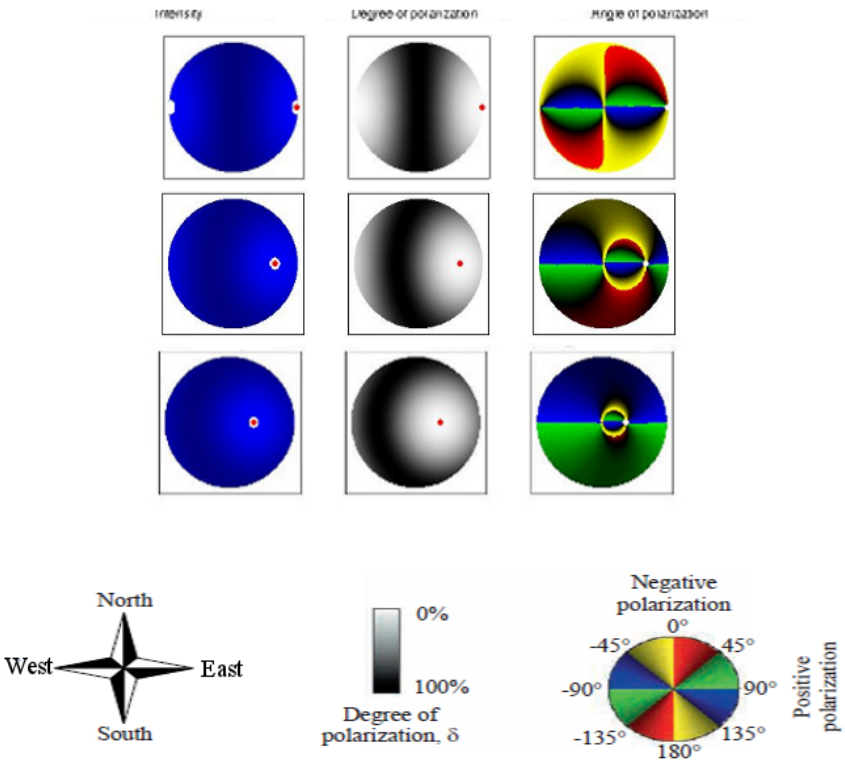

Figure 4.5: Example of polarization patterns in the sky, for three different elevation of the sun (red and white circles)

single photoreceptor responds when pointing to different patches of the sky. The program has also an ephemeris function based on [**?**] for computing the solar position during a specific day, for a specific longitude and latitude. The tool is implemented in Matlab [] and the main trigonometric functions are computed using cosd,sind and tan2 functions to overcome numerical problems and provide major stability for particular input values, such as $\frac{\pi}{2}$ or $-\pi$.

From figure ... it's possible to observe that the intensity and the degree of polarization are mirrored with respect to the solar and antisolar meridian and the degree of polarization is maximum at a radial distance of 90°, along the North-South axis and the intensity is maximum in proximity of the sun and on the opposite antisolar point, while is minimum at a zenithal distance of 90°, following a distribution inverse to the one followed by the degree of polarization.

The angle of polarization is always perpendicular to the plane of scattering formed by the zenith,the observed point and the sun. If measured with respect to the local meridian ,angles of 90±45 °correspond to a direction (green and blue shaded area in the picture) of polarization almost orthogonal, while angles

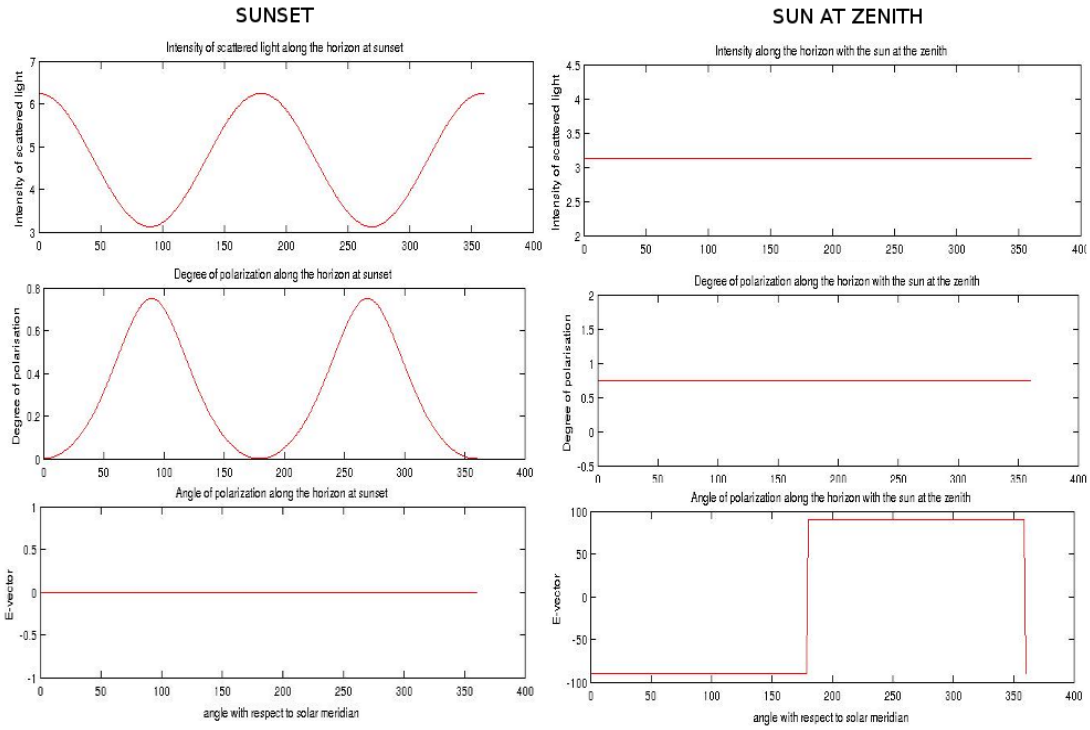

Figure 4.6: Example of polarization patterns along the horizon, for all azimuthal angles,at two different sun elevation.

of 0±45 °corresponds to direction of polarization almost parallels to the local meridian [**?**].

Consider for instance figure 4.5. At low solar elevations, near the sunset ,the e-vectors are orthogonal in proximity of the zenith and along the east-west axis, while the polarization is strongly parallel in the rest of the skydome. As the sun rise and approach the zenith positive polarization largely increase to reach the maximum when the sun is at the zenith. To better understand the pattern of polarization , in figure 4.6 we can see the distribution of the light intensity, degree of polarization and angle of polarization along the horizon at sunset and when the sun is at the zenith. At an elevation of 0°intensity and degree of polarization vary in a sinusoidal way depending on the azimuth angle, and the angle of polarization is always parallel to the local meridian,meaning that shift progressively with respect to the zenith as the azimuth shifts. When the sun is at the zenith the intensity and degree of polarization are constant along the horizon, as the patterns of polarization are distributed in concentric circles. The angle of polarization is always perpendicular to the local meridian, at -90 or 90 °, depending if on the

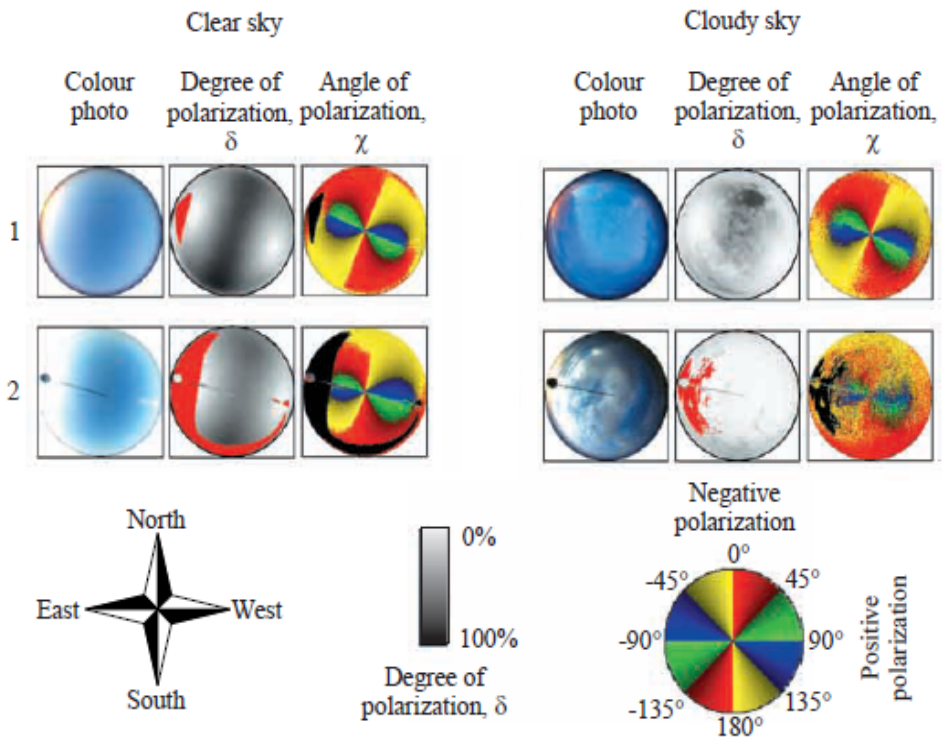

Figure 4.7: Example of polarization patterns from a polarimetric study,for two different elevation of the sun,under a clear(left) and a cloudy (right) sky. Compare with the simulated sky. From [**?**]

solar or antisolar part of the sky. We can also notice the simmetry of the signal with respect to the solar meridians. The model implemented is an approximation of the real sky polarization, as measure in various polarimetric studies (e.g [**?**, **?**] and it best approximates clear sky conditions. Hazing phenomena , occlusion by the clouds , urban pollution , aerosol phenomena are not taken in consideration by the model, as well as the non linear component of the polarized light. In this case it's better to use the Mie scattering equations. Also, there are some points in the sky, in particular the Arago and Babinet point when the degree of polarization is 0 and the model it's not able to describe them (see figure real sky). However,for the purpose of providing a more realistic input to the simulated photoreceptors and eliminate ,at least at the beginning, noisy factors from the subsequent analysis the simplest choice of the Rayleigh sky model seemed sufficiently reasonable.

4.3 Photoreceptor simulation

A single ommatidium in the compound eye of the insect is a complex optic device which measures the amount of incident light reaching its field of view. From a theoretical point of view an ommatidia can be seen as a multi-mode waveguide []. Specialized photoreceptors in the DRA exhibit a high grade of polarization sensitivity (PS) in the UV or blue band of thespectrum and almost no response to unpolarized light. Specific level of PS vary across the species , but on the average assume a value of to 10 in the DRA, while are usually 2-3 in the remaining part of the compound eye []. Polarization sensitivity is highly determined by the alignment of the block of rabdhomers and by the dichroic ratio, the proportion of rabdhomere arrangend in different directions. In the ommatidia of the DRA the microvilli are oriented in two mutual orthogonally directions, enhancing the sensitivity of the photoreceptor. The optical axes with respect to the body axis determine the angle of polarization at which the photoreceptor exhibit maximal response.

A complete simulation of a single ommatidia would require complex optics computations ,a more sophisticated modelling of the radiance distribution adding a considerable amount of computational load on the entire simulation. The key point is that a single ommatidia act as an analyzer with two antaghonistic sinusoidal response to different e-vector orientations.

4.3.1 Single Photoreceptor

At the beginning of the project the response function for a single photoreceptor s was modelled as:

$$r(\alpha) = CI(1 + d\cos(2\alpha - 2\alpha_{max}) \tag{4.7}$$

where I is the intensity of the scattered light, d the degree of polarization, α the e-vector orientation ,α_{max} the e-vector orientation eliciting maximal response and C a scaling constant. I,d and α are computed, for each point of interest, using the values provided by the Rayleigh sky model. For each photoreceptor (simulated ommatidia) two functions are computed, one for α_{max}, which represent the main optical axes and one for $\alpha_{max} + 90°$, the orthogonally oriented microvilli.

The formula developed by Lambrinos [] described the response of the sensors mounted on the Sabahot robot to the azimuthal angle of the main axis of robot with the solar meridian. The response curve of the original model is hence a

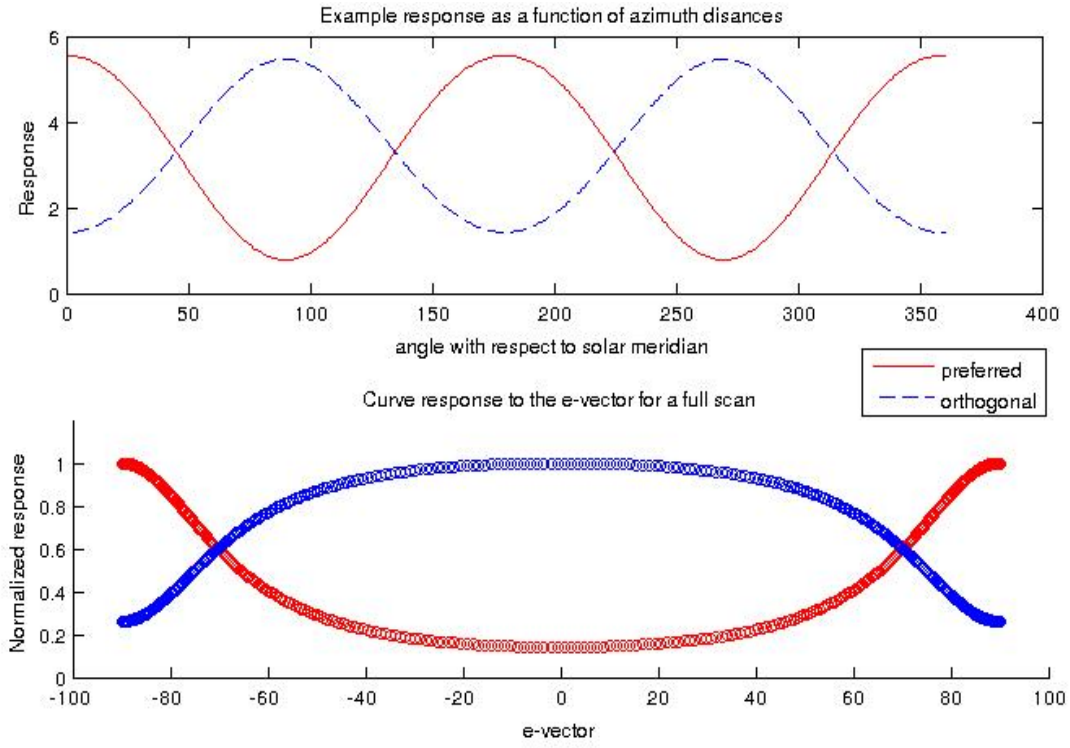

Figure 4.8: Example of the response of a simulated photoreceptor with preferred orientation 0°as a function of azimuthal angles, during a full 360°rotation

sinusoidal function of azimuthal distances, as showed in figure 4.7, for a solar elevation of 0°and a point at polar coordinates $p(0°, 70°$ during a full 360°rotation. However, since photoreceptors respond to e-vector orientation and the interest was in explorying how to compute the azimuthal angle from the single ommatidia response, we consider the input to equation 4.8 as the angle of polarization. In particular this generate a more shaped and narrower (hence more selective) tuning curve for the e-vector response and permit to replicate some lab experiments,such as a single rotating polarizer, useful when experimenting with neurons.

The response of the same photoreceptorthe using the e-vector as input during a full rotation is showed in figure 4.10. As we can notice the response is always sinusoidal , but there is a less pronounced selectivity with respect to azimuthal distances and more selectivity with respect to the e-vectors. The main axis of the sensor is oriented at 90°and the responses of the two microvilli are inverted if compared to the model with azimuthal angles as input. Indeed when aligned with the solar meridian, as in this case, the e-vector is orthogonal to the local meridian while the azimuthal angle is ,of course, 0°. However the simulated agent has to

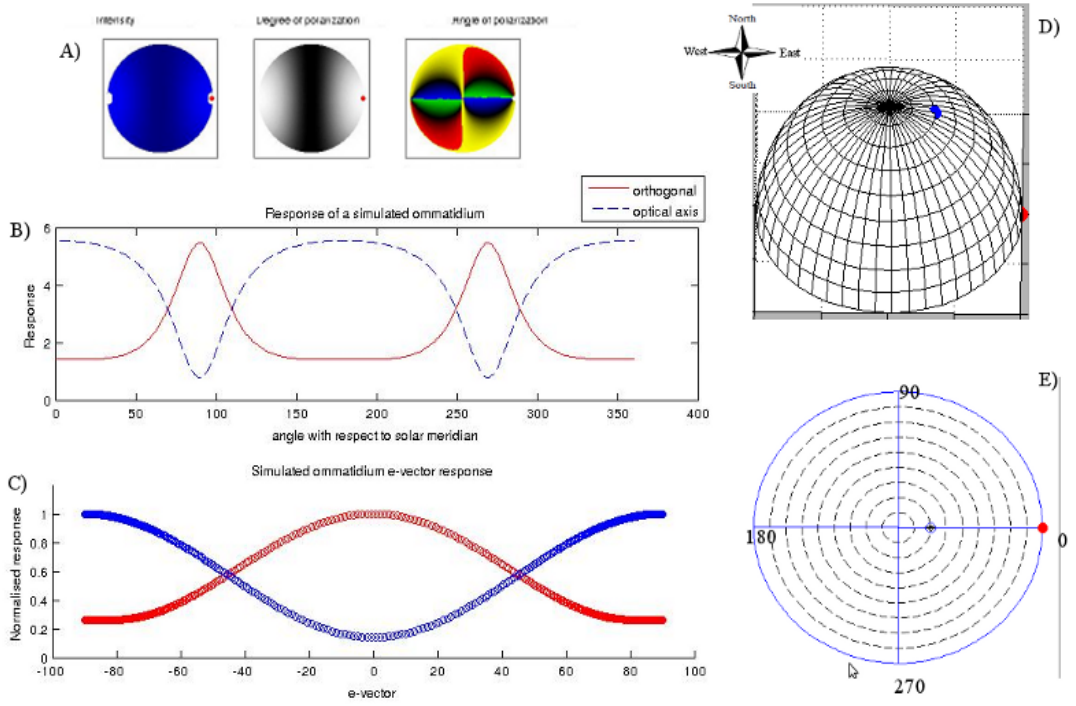

Figure 4.9: Example of the response of a simulated ommatidium with optical axis at 90°during a full 360°rotation. a)polarization patterns b)response c)tuning curve d) 3d view of sun(red circle) and observed point (blue circle). e)2d view in polar coordnates

take into account the relative displacement of the sensors with respect to the main axis and , if computing an absolute vector in egocentric or geocentric coordinates, translate the single signals accordingly. This add a major level of realism to the simulation, even if the two inputs, threated carefully, have the same meaning. Experimenting with the model however we discovered a problem. From eq. 4.7 it's easy to observe that a single rhabdomere modelled in such way is highly sensitive to change in the intensity of the light and that amplitude modulation and polarisation opponency will depend highly on the elevation of the sun, the point observed and the preferred orientation. The response is linear with respect to either degree of polarisation or intensity for a given e-vector. This means that simulating a rotating polarizer in a lab environment the modulation will depend largely on the e-vector orientation. However neither of this quantities remain constant during a rotation under real sky (even in this highly simplified model). When the e-vector is approximately constant along the arc described by the

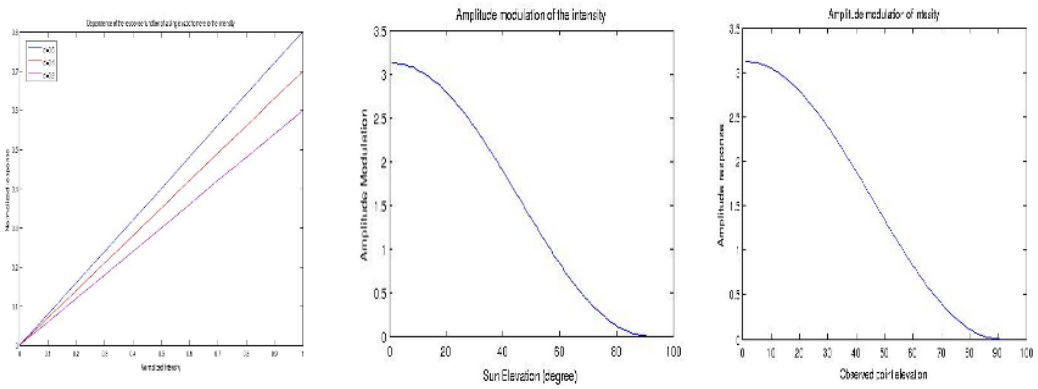

Figure 4.10: Dipendence of the response to the intensity of scattered light.

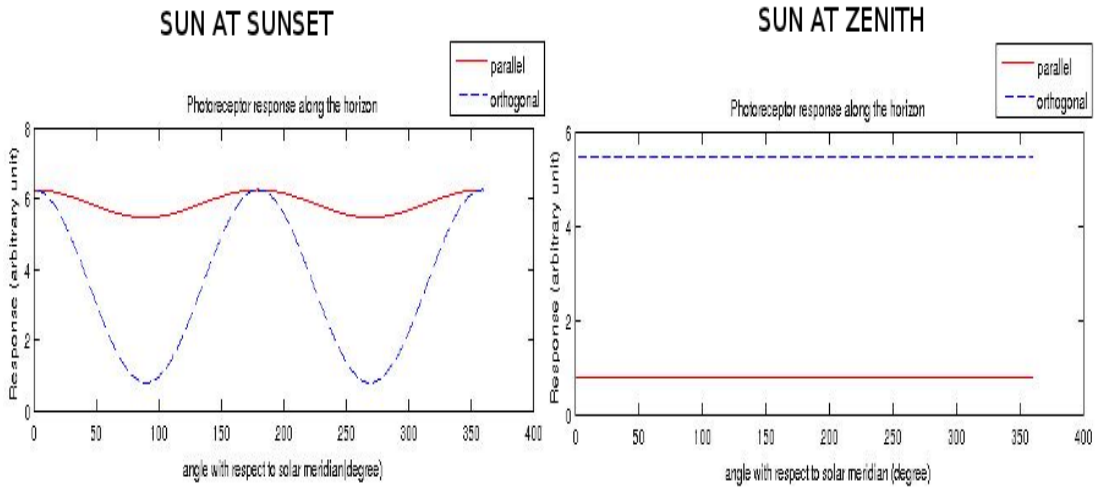

Figure 4.11: Response of the two orthogonal photoreceptors along the horizon, during a full rotation, at sunset (left) or at the zenith (right).

simulated rotatory movement and it's parallel to the optical axis, the cosine term in 4.7 will dominate, as intensity and degree of polarization are out of phase and the response will be high and approximately constant. However, in this case, the orthogonal optical axes will be near the minimum and eq 4.7 is dominated by the modulation of the intensity. If the amplitude response of the intensity modulation vary largely during the movement the response of the photoreceptor will be highly variable, even in the presence of constant e-vectors. Consider for instance the two cases described in figure 4.9, for an ommatidia at an elevation of $\theta = 0$. At sunset the e-vector along the horizon is constant , while intensity and degree vary largely depending on the azimuth angle (see fig 4.6). Hence the photoreceptor with optical axes parallel to the local meridian will have a high response and the

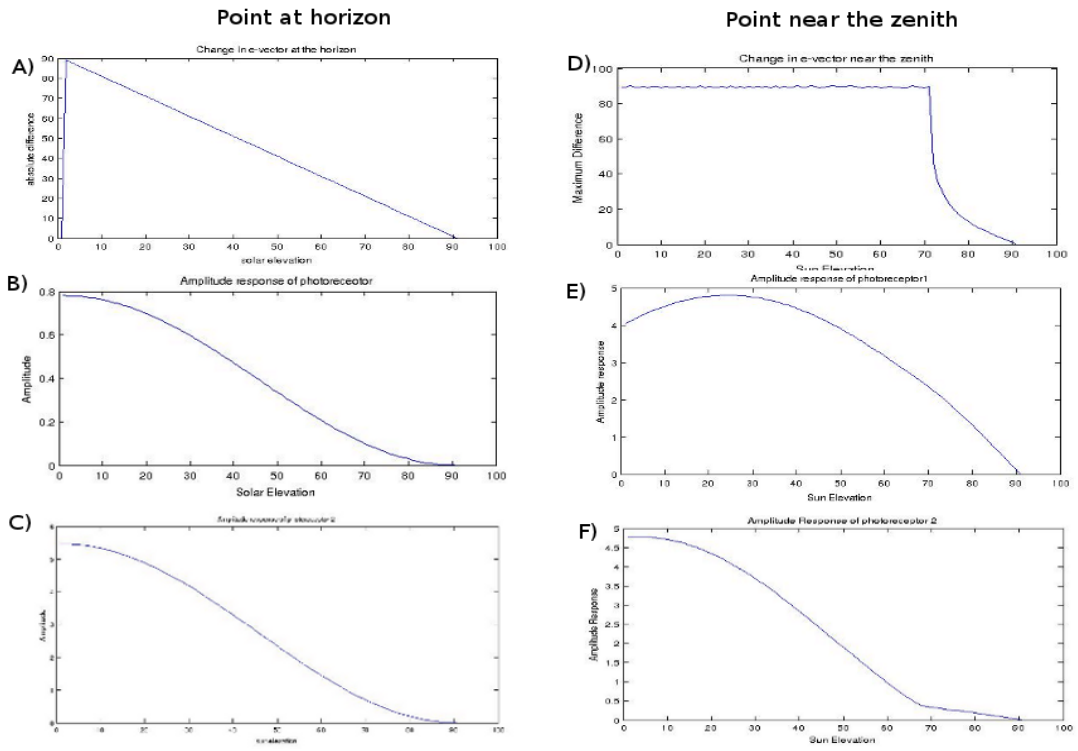

Figure 4.12: Illustration of variabilit and accuracy in the amplitude response depending on the observed elevation. A-C: observed point at the horizon. D-F: Observed point near the zenith, $\theta = 70$.A,D: Maximum difference in e-vectors for each increment (1 °) during a full 360 °rotation as a function of solar elevation. B,E : Response of photoreceptor 1 (parallel microvilli) during the rotation. D,F: Response of photoreceptor 2.

influence of the intensity is minimal. For the orthogonal optical axis however the cosine term is alway at minimum, but due the high variability in intensity, the response is misleading. On the opposite, with the sun at the zenith, intensity and degree are constant for a concentric circle and the response is constant for both photoreceptors. The amplitude (difference between peak and minimum activity) of the intensity change with the elevation of the observed point and is less pronounced as we approach the zenith, indipendently of the solar elevation (figure 4.). This means that the effect of intensity is less pronounced near the zenith, as we can see from figure 4. . The figure shows a comparison of the e-vector variability and the response of the two photoreceptors of a single ommatidium , for two different observed elevation, at the horizon and near the zenith, during full rotations of 360 °and for different solar elevations. For the point at the

zenith the e-vector variability descrease as the sun increase its elevation. Despite this fact, the photoreceptor with parallel microvilli has a very small amplitude response as both the e-vector but also the intensity descrease their amplitude response with progressively solar elevation and the combination of the variables is balanced at every solar elvation. What changes in this case is the absolute peak response, the offset of the modulation which decrease as the sun is near its peak. In this case indeed the e-vector is parallel only at the sunset,and along the horizon the polarization is negative for most of the azimuth angles (even if the absolute amplitude response is high, since there are pints with high positive polarization) , so the photoreceptor receive for small solar elevations an-evector similar to its preferred orientation and the cosine modulation dominate. With increasing sun elevation the polarization progressively shifts to positive values along the horizons and the response is dominated by the intensity modulation. But at that point the intensity variation is less pronounced and the amplitude modulation remain low. Conversely the second photoreceptor (orthogonal microvilli) has always an high modulation ,because the progression is exactly inverse.

For a point near the zenith instead , since the intensity modulation is smaller, the information provided by the photoreceptors is most accurate and depends more on the single e-vectors.

The excessive dependence on the intensity ,the failing in explaining the polarisation sensitivity of the photoreceptors and the low dependance on the degree of polarization was judged inadequate to the simulation of the ommatidia. When the degree of polarization is low indeed , the response of an ommatidia should be absent or very low, as testified by the electrophysiological recordings of recorded UV cells and pol neurons in crickets [**?**]. A simple solution which not required a more appropriate, but time consuming optical simulation, was founded adapting the work of Glas [**?**]. The revised photoreceptors response was modelled as

$$r(\alpha) = CI + dPS\cos^2(\alpha - \alpha_max) \tag{4.8}$$

where C is a constant of scaling, I the intensity of the scattered light, d the degree of polarization ,PS the max polarization sensitivity of the photoreceptor and α and α_max defined as above. In this way the response is more strongly dependent on the degree of polarization and better capture the response of a single UV cell. As we can see from figure 4. ,describing a full rotation along the horizon at sunset, the photoreceptor with maximal response at 0°is now correctly modulated by the

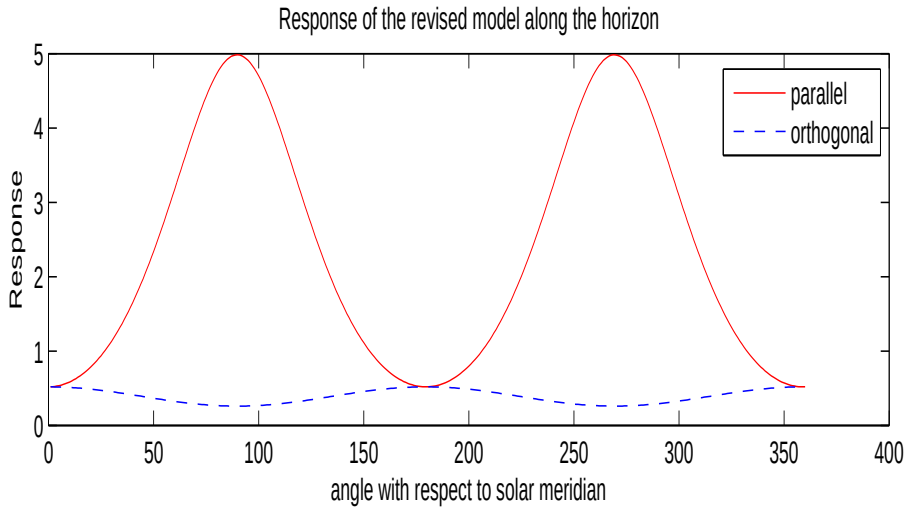

Figure 4.13: Revised photoreceptor model.

degree of polarization and the photoreceptor with orthogonal direction is only lightely modulated by the intensity of the scattered light.

4.3.2 Simulation of the DRA

As discussed in Chapter 2 , the ommatidia in the DRA forms a series of analyzers used to sample different patches of the sky and send information about specific e-vectors to the optic lobe. In crickets the ommatidia come arranged in a series of semicircles with three classes of similar preferred orientations and overlapping field of view, while in ants there is a characteristic fan style distribution with more variety in the arrangement of optical axes (fig. 2.2).

To simulate the arrangement of different ommatidia I added an extension to the GUI developed for the single ommatidia, to facilitate the task of adding and monitorate the various photoreceptors .

The simulation tries to mimick the sensory system of ants and crickets. To simplify the modelling only a subset of the ommatidia were used and for crickets I didn't reply the semicircular patterns. The hypothesis was that the main difference comes from the coarser,overlapping larger visual field in crickets and from

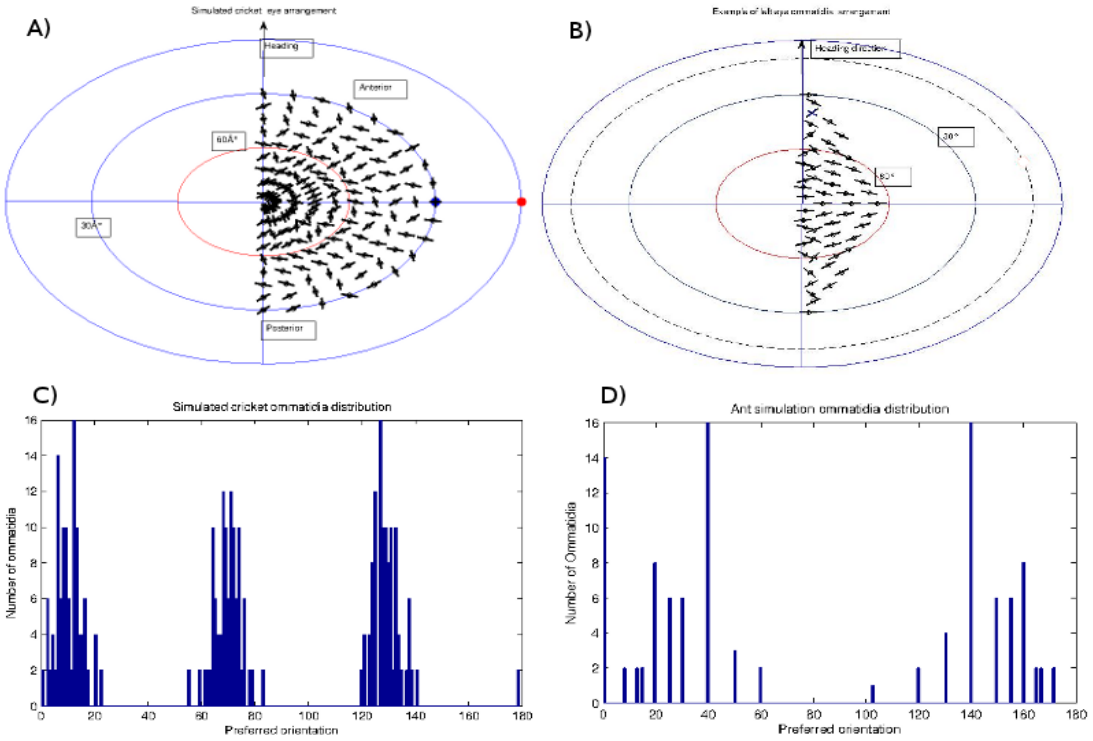

Figure 4.14: Arrangement of the ommatidia of two different DRA, one resembling crickets and the other resampling ants.Only the left eye is provided. A)Cricket B)Ant C)Distribution of preferred orientations in the simulated cricket D)Distribution of preferred orientations in the simulated ant

the existence of three well defined class of preferred distribution. In ants instead the ommatidia are more spaced with narrower field of view (approx. 5°) and without a clustering of preferred orientations. The DRA area of crickets extends up to 60 °from the zenith, at elevations of 30°either in the anterior-posterior axis (the main body) and to the left and right. The DRA of ants is smaller and clustered around an aerea of 30 °around the zenith, for each eyes, with only a small portion in the anterior and posterior part sampling elevations of up to 30 °. The ommatidia of the ant were added manually , while for the cricket's ommatidia the arrangement was generated by a script. The script ensures that there are three set of photoreceptors with parallel axis and different preffered orientations,pointing at similar pathces of the sky. The set of preferred orientations was generated picking from three gaussians distributions with means 10 °,70°, 130°respectively and a standard deviation of 5, sampling at azimuthal angles of 10°and elevations of 7°. The simulated DRA of ant contains in total 110 ommatidia, 55 for each

emisphere, while the simulated cricket has 342 ommatidia in total. A PS value of 6.3 was used for the ant's ommatidia and a value of 10 for the crickets one.

The artificial DRA was tested during full rotations at different levels of solar elevations. To simplify the experiment I assumed the azimuth of the sun constant during its rise towards the zenith and the insect starting aligned with the solar meridian. As expected a correlation test revelead an high dependency on the evector variability, for all ommatidia , in both the simulated insects (p-value ¡0.002), with high dependencies also on the degree of polarization.

The mean amplitude response of the ommatidia was higher at lower sun's elevations, while progressively reducing with the sun near the zenith, when the degree of polarisation is lower and constant along circles of equal elevation. The amplitude response was generally more pronounced in the periphery of the DRA,with higher negative polarization on the average, while more stable near the zenith. For both insects near the zenit the response is more homogeneous than in the periphery. As the sun rise, the degree of polarization is higher in the zenithal regions and so there is a more pronounced response of the receptors pointing in that area,but at higher solar elevation, with an increase in the intensity of the light, the situation is the opposite. The main difference between the two animals, for the case considered, emerge in the polarization opponency of the antaghonistic photoreceptors. Under the same sky conditions ,the alignement of the photoreceptors generate a very different progression. For ants there is a higher response of microvilli with parallel orientation at lower elevation in the periphery of the DRA, more sensitive to negative polarization; as the sun rise insted we observe a major excitation in the central photoreceptors. For crikets instead, on the average there are no differences among the different areas and there is a major excitation at low solar elevations, and a progressive increase in the response of orthogonally arranged microvilli at higher elevation. In all cases the contrast is higher in the central photoreceptors of the DRA, since there is a more pronounced positive polarization near the zenith and more variability along the peripherical zones. As a consequence based on the elevation of the sun ants in particular seems to have a major variability in the responses of their photoreceptors.

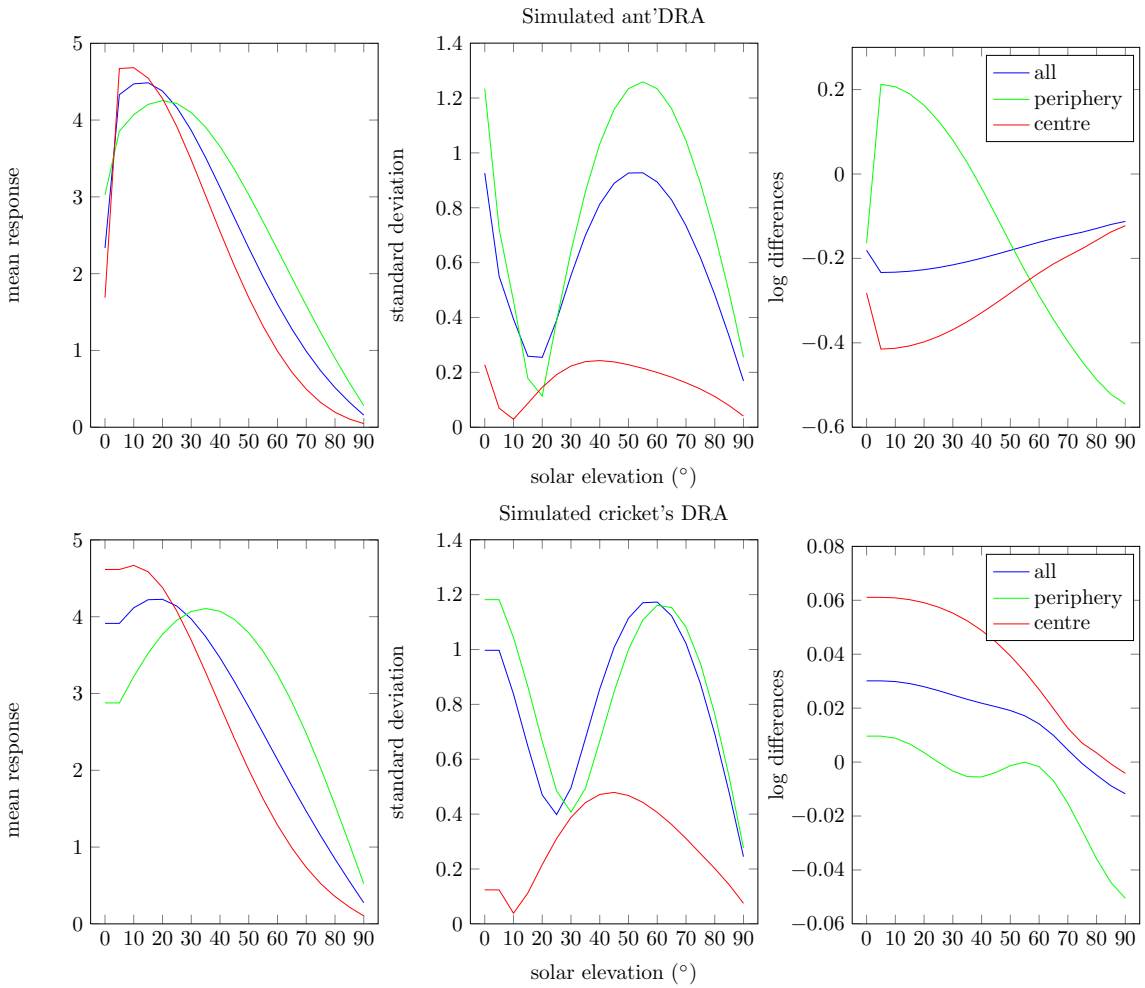

Figure 4.15: Average response of the DRA sensors's during full rotations, at different solar elevations. Top row: Ant's DRA. Bottom Row: Cricket's DRA. Left: Mean amplitude response of ommatidia pointing near the zenith(red), at the periphery of the DRA (green) and combined. Center: variability of the mean amplitude response. Right: Polarization opponency, measured as the difference of the log of the signals of the two photoreceptors in one ommatidia. Average values.

4.4 Summary

In this chapter I have exposed the work done in modelling the input stage of processing necessary for polarization compass and path integration. Due to problems in the sensors a Rayleigh simulation of the skydome has been provided , as well as a simple simulation of the response of single ommatidia. The system illustrate the basic concepts involved in vector navigation in insect, but it's a simple and limited model which can be extended to provide more realistic informations. A better simulation of skylight can be implemented for instance using the models described in [**?**, **?**] which take into account also second and third order scattering phenomena. Another possibility would be to use a neuromorphic device as in [] or collect the data using a polarimetric device, such a fish eye lens with a polarization filter [].

Having a complete model of the irradiance ,for the realism of the model a waveguide simulation of single of ommatidia would be beneficial. The example considered indeed it's an over simplification and it's not able to capture spatial properties and diversity of single ommatidia, noise in their response, difference in PS, absolute sensitivity and influence of the field of view. Using the work of [**?**, **?**, **?**, **?**] it would be possible to provide a most accurate simulation. To fulfill computational complexity requirements of such navigation a distributed process of the simulation should be adopted.

As a third alternative would be to use an artificial compound eye mounted on a real robot [**?**, **?**].

The analysis provided is hence just an exemplification of the possible scenario that the sensory periphery has to face under (idealized) sky conditions. The responses will vary according not only to the solar elevation but in relation to geographical location and epheris function of the sun. The simulation is not aimed to provide an accurate and quantitative prediction of the sensory periphery of the DRA. The key point is that according to the sun's position different area of the DRA are most active and reliable, and this must be accounted by a filtering of the signal or by a mechanism of selection of the most reliable information, by a comparison of the response coming from different areas.

Chapter 5

Modelling Polarization Sensitive Neurons

In this chapter I discuss the attempt to modelling the pol neurons founded in the optic lobe of arthropods, to explore possible dynamics of neural integration of pattern of polarization in the sky and provide a more realistic input to subsequent layers implementing polarization compass and path integration or integrate the system with pre-exsisting models.

In the first section I briefly discuss the neuron model choosed, than in section 4.2 the statistics used for modelling and the types of test conducted. Section 4.3 shows the result of modelling a single pol neuron, while in section 4.4 I present the model for the complete optic lobe.

5.1 Neuron Model

Biological plausibles neuron models are computational and mathematical description of the dynamics that lead the membrane potential of a neuron to change it's rest state in response to an input (in the form of a current or a voltage). When the neuron reach a certain voltage threshold there is a sudden peak in the membrane potential and the neuron is said to fire (produce) a spike [**?**, **?**]. After the spike the membrane is hyperpolarized and returns to a value similar to its rest potential,with the property that it will be more difficult to lead to a new spike immediately after the previous one (refractoriness). A spike, or a train of spkes, are considered as the fundamental computational unit for a single neurons. Differently from artificial neural networks such as the perceptron and the

multilayer perceptron, in which a spike is threated as a 0-1 event , biophysical models attempt to describe the internal dynamics of the membrane potential and the time course of inputs and spike generation. The so-called neural newtork of second generation consider a more realistic alternatives and describe the neurons in terms of activation functions depending on the firing rate of the input neurons and the weight of the connections. However firing rates are not the only important characteristic of spiking neurons and most important are the time dynamics of the model, as well the time of spiking and the characteristic of the train of spike produced by a neuron have fundamental information theoretic content and properties. To complicate things also the synapses and dentrites, the junctions by which neurons are interconnected, have important temporal characteristics that influence the behaviour of a neurons and are not merely weights indicating the strength of the connections []. So when we want to study the neural dynamics of real organisms it's important to resort to more plausibles approximations. The main problem is that networks of spiking neurons are not generally amenable to mathematical analysis and numerical simulation must be adopted. There exists a great variety of models of single neurons and neural dynamics [**?**], among the which the Hugley-Hoxey [] model is to date the most important and realistic model, describing in terms of four coupled differential equations the precise dynamics of the membrane potential and the ion channels that influence the voltage of a neuron. However the Hudgley-Hoxley model has an high computational cost , requiring approximatively 1200 floating point operations for a single 1ms of simulation. Among the models based on differential equations (an alternative is the SRM model of Geinsteiner, which express the dynamics in terms of filters) the Izhikevic model [**?**, **?**] is one of the most advanced model, and the only one being able , with a suitable choice of parameters, to emulate all the spiking dynamics of the Hudgley-Huxley model, but with the same computational efficiecy of another popular neuron model, the integrate and fire [**?**].

The Izhikevich model is based on the bifurcation theory [**?**] and phase-plane analysis and it's a dynamical systems based on two ordinary differential equations:

$$\frac{dv}{dt} = 0.04v^2 + 5v + 140 - u + I \tag{5.1}$$

$$\frac{u}{dt} = a(bv - u) \tag{5.2}$$

where v represent the membrane potential ,u a recovery variable describing the ionic currents and t the time. I describes the currents reaching the soma in input, a and b describe the time scale and the sensitivity of the recovery variable , c the voltage reset and d the after spike reset of the recovery variable. The after spike reset of the model is described as:

$$\text{if } v >= 30 \text{ then } \quad \begin{cases} v = c \\ u = u + d \end{cases} \tag{5.3}$$

For the input currents a constant input current was used to simulate background actvity, probably derived by feedback connections, while for the synaptic connections the simulation employed conductance based models with exponential decay [**?**, **?**, **?**]. A single synapse in this model has the form:

$$g(t) = g_{syn} e^{-\frac{(t-t_0)}{\tau}} \tag{5.4}$$

where g_{syn} is the maximal conductance. In this model the synapse is assumed to suddenly increase it's voltage from 0 to g_{syn} and than decay with time τ. Another more sophisticated model could have been an alpha synapse, even if, exponential synapses are suitable for fast synapses on a thin dentrite and certain type of inhibitory (hyperpolarizing) synapses [**?**] and are largely used in simulations. A suitable choice would depend by the specific neurotransmitter of the modelled neuron. When a synapse is active it acts as a source of current by :

$$I_{syn} = g(t)[v(t) - E_{syn}] \tag{5.5}$$

where E_{syn} represents the reversal potential of the synapse and v(t) is the membrane potential of the postsynaptic input. The total current reaching a neuron is the sum of the single currents. In this model we ignored delay propagation and dentritic filtering [**?**]. A simpler solution would have been to make the synapses act as a current source instead of an ohmic conductance [**?**]. With the first experiments on the model a problem emerged, expecially with voltage-dependent synaptic current. The problem was that the equation 5.1 in the Izhikevic model is not bounded and the voltage can stagger over 30 mV. This in turn make the synaptic current grow or decrease to unrealstic high values and also modifies the kinetics of the reset variables.

The first solution was to simply bound the equation peaking $v(t) = min(30, v(t))$.This already solved the problem and doesn't inficiate the model dynamics, as the voltage is not supposed to However Wang [**?**] proposed a similar but more refined

version that avoid staggering of peak voltages and bound the equations, taking into account also the previous values of the membrane potential. In the simulations we adopted this improved version. The parameters for the neurons has been set to simulate integrators or class 1 excitability behviours. Both type of neurons respond with tonic spiking when stimulated and their spike train is suitable to encode the strenght of the signal. There are other possible representations , such a phase coding in the Fourier dimension [] for which resonators would have been more suitable. However from the electrophysiological recordings [] emerged the modulation of firing rates depending on the particular e-vector, so integrators seemed appropriate.

5.2 Methods

To experiment with the neuron model and develop a simulation of the optic lobe I started modelling a single neuron receiving antaghonistic input from the pair of photoreceptors in the ommatidia. Three conditions in particular were examined:

- Single stimulation: In this case the neurons don't receive external stimulus for a while and than an e-vector is presented to the photoreceptors for relatively short time intervals, (200-500 ms) , and than the stimulus is removed. Intensity and degree of polarization are assumed to be constant during the entire stimulation. This case of study is useful to observe the response to single e-vectors with respect to the background activity and for setting the parameters of the neuron.

- Continuous rotating polarizer: As before intensity and degree of polarization are assumed to be constant (simulated lab conditions) but the e-vector is continuously rotating from 0 to 180 or 360 °. This case of study is similar to the experiments conducted for electrophysiological recordings and can be used for comparison with literature finding and to optimize the parameters.

- Simulated skylight: In this case the neurons receive a stimulation (static or continuous) under the Rayleigh sky model of polarization. This case of study is useful to formulate hypothesis on how the polarization compass can be solved by spiking neurons and to provide indications to be cofirmed with electrophysiological recordings. In this case is better to observe the behaviour of the entire network.

The strategy to model the neurons was to collect statistics and , in the majority of the case, conduct a simple automated or manual curve fitting to vary the parameters and observe the response. The reason for this choice was that at a first instance we don't know what specific computational process a certain group of neurons are performing, and so it's not clear which kind of optimization should be conducted. A mathematical based approach is not alway possible with spiking neurons, expecially when the connections are dynamics and moreover not even the topology of the network was specified. An exploratory approach seemed the best choice at the beginning of the project, even if , as discussed in the final chapter formulating some hypothesis on the functional role of the different areas of the brain and trying to optimize in this regard could have been a possible alternative. In particular due to the absence of a proper dataset and faced with published results from different anymals the idea of experimenting and try to find useful insights seemed reasonable, and it is not uncommon practice in computational neuroscience []. Another alternative, using an evolutionary multi-objective process [] has been defined and evaluated , expecially for the case of tangential neurons. But mainly due to the delay in modelling of the early sensory stages, and due to the time required to collects suitable data with a reasonable number of neurons and layers of the network, this road was abandoned for trying to integrate the model with pre-exhisting models.

For the majority of the experiments the statistics observed were:

- Response amplitude and modulation: One of the main characteristic of polarization sensitive neurons is that they modulate their activity when stimulated by single e-vectors and the modulation is periodic with period of 180 °. The amplitude of the modulation varies across the species [] and characterize also neurons of the same organism present in different areas of the brain and with different morphology. The response modulation is computed measuring the firing rates in a certain time span. In the case of static stimulation the firing rates were measured in absence or in presence of the stimulus. With continuous rotating polarizer , as done in [] for real neurons, the activity were divided in overlapping bins and the firing rate computed within each bin, usually in a time span of 1 sec.

- Response Fitting: To characterize the entity of the response modulation, the firing rates with respect to different evectors were fitted to a $\sin^2$ or $\cos^2$

curve using the Levenberq-Marquardt algorithm [].

- Peak activity: The point of peak activity it's used to define the preferred orientation of the polarization sensitive neurons. Peak activity was founded searching for the point of absolute maximum in the firing rates and compared also with the point of maxima founded by the fitted response. In case of good fitting and multiple maxima the first one (as the function is periodic) was used to characterize the preferred orientation.

- Background activity: characterize the activity of the neuron in absence of stimulation. It is useful to determine the amplitude modulation and to model neurons with different characteristic. In the early stage of processing neurons have a reduced background activity, indicating that are not involved in a variety of activity, while, at least in the brain of the locusts, neurons in the later pathways have a higher background activity and less amplitude response, suggesting a possible role of integration of sensory information.

- Mean activity: In the case of a continuous stimulation the mean firing rate across all bins was collected, to determine the background actitvity during a tonic spike train.

- Connectivity: The number and type of neurons sending pre-synaptic input was utilized to explore the possible functional role of a certain neuron. Depending on the pattern of connectivity we wanted to observe the characteristic of a response and formulate hypothesis on the possible adavantages of certain topologies.

- Field of view: The connectivity of a neurons determine also the area of the sky from which a neuron is receiving information. Different neurons have different field of view and can receive input from the ipsilateral emisphere, the contralateral or both. In the brain of locusts neuropils of different area have different field of views and this is a possible indication of their functional role.

- Tuning widths: The tuning widths represent the range of e-vectors eliciting maximal response or response over a certain threshold. In the brain of locust for each typoe of neuron there are specific tuning widths and , adopting various pattern of connectivity we wanted to try to match the

tuning widths of specific neurons, to characterize their role in signal processing. Moreover tuning widths under real sky conditions have not been recorded and the simulation could provide some interesting insights (with the obvious limitations due to the approximation of the simulation). Neurons with narrower tuning activity are most selective to e-vectors and are most likely assumng the role of compass neuron, while neurons with wider tuning widths probably integrate signal from various photoreceptors or are involved in integrating other information with the polarization signal. A bell shape tuning width is typical of neurons processing sensory information and has been found in the rat's cortex [] but also in the visual cortex of monkeys [] for example. These curves are characteristich of perception. For different group of neurons the tuning witdhs are computed as in [], aligning their maximum response to a [-90°,90°] , with 0°representing the preferred orientation.

5.3 Single neuron

The signal received from each of the two photoreceptor in an ommatidia is considered as a source of voltage and converted to a current using Ohm 's law. For the simplest case, a single neuron receiving anthagonistic input from a single pair of phoreceptors has been studied. A single pol neuron of this type could also be used to process the information of sensors width wide field of view, such the polarization sensors adopted in the Sabahot robot, without the need of modelling the sensory periphery. For each neuron n receiving input from a single ommatidia (under stimulation), the presynaptic input current I in 5.1 can be described as :

$$I_n(t) = I_{back} + \sum_{i=1}^{2} \frac{r_i(\alpha_t)}{imp(i)} \tag{5.6}$$

where $r_i(\alpha_t)$ is the response of a single photoreceptor as in 4.9,α_t the stimulus at time t , and I_{back} is a current used to simulate background activity and feedback connections, or to shape the behaviour of the neuron according to the electrophysiological data. Imp(i) represents the value of impendance used to convert the response of the photoreceptor to a source of current.

The response of a neuron to a single e-vector presented in the time window

$[t_s, t_e]$ can be quantified as :

$$s(\alpha) = \sum_{t=t_s}^{t_e} \delta(t - t_i) \tag{5.7}$$

where δ is the Dirac function and t_i the time at which the neurons spike in the time window considered, $t_i \in [([t_s, t_e\ ]$. Alternatively the response can be quantified using the average interspike interval :

$$isi = \frac{1}{n} \sum_{i=2}^{n} t_i - t_{i-1}, n \geq 2 \tag{5.8}$$

$$s(\alpha) = \frac{1}{isi} \tag{5.9}$$

The average interspike interval measure the average time that occurs between two consecutive spikes , in a spike train of n spikes. For a sufficient number of samples it represents a better measure of the firing rates than simple counting [], as it is an indication of the probability that a neuron will fire a certain number of spikes in a certain interval. Finally we can define the amplitude response as:

$$a(\alpha) = s(\alpha) + w \tag{5.10}$$

where w is the background activity of the neuron.

5.3.0.1 Static Stimulus

The first experiment was to observe the response of a single pol neuron to a static stimulus of 200-300 ms. The parameters of the Izhikevich neuron were a=0.02, b=0.2, c=-65,d=8,v_{rest}=-65 . The ommatidia providing input was choose with a preferred orientation of 0 °.

The minimum background current to let a neuron spike with this parameters is 1, and the relation with the background activity is linear. The current acts as a scale factor on the amplitude modulation, but if sufficiently high and excitatory doesn't affect too much the shape of the response to a single pair of photoreceptors. In this case we fixed the input current to 5 and provide a low background activity of 7-10 spikes. There is no single value of current adapt to model all neurons of different species, as their background activity is variable. For example Labhart [] reported an absence of spontaneous activity for crickets, while in ants the spontaneous activity was quite high [] .

From figure 5.2 we can clearly see that an integrator responds tonically when stimulated by an ommatidium and modulates it's background amplitude encoding the antagonistic signals of the two photoreceptors. We can also appreciate that

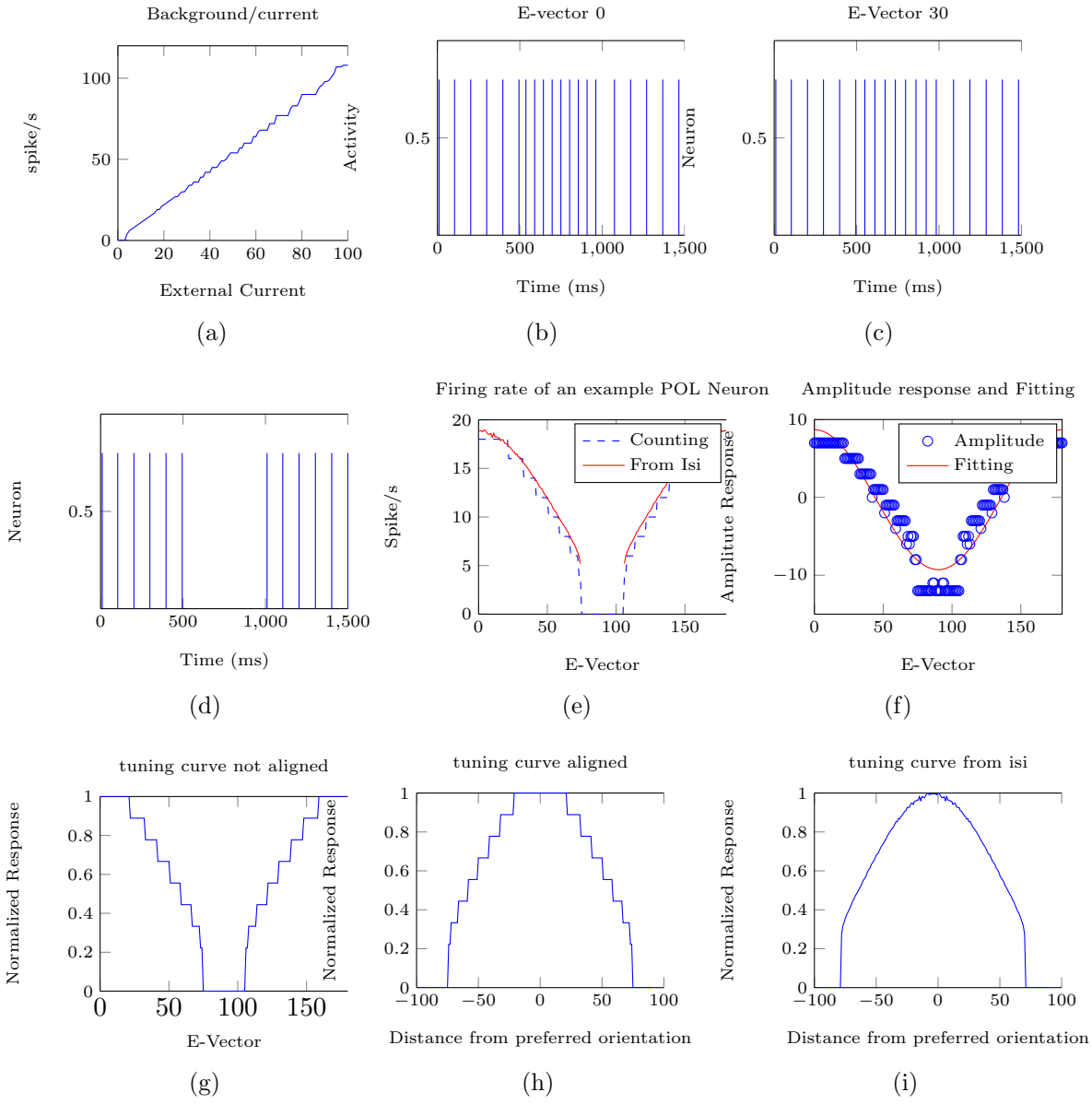

Figure 5.1: Experiments on a single pol neuron

firing rates estimating using ISI produce a smoother curve and capture better the variability in a single spike train, as the time to spike is not considered by simple counting. The fitting to the amplitude modulation is almost perfect. For the Levenberg-Marquardt algorithm the function to fit was

$$f(\alpha) = x_1 \sin(x_2 - \alpha)^2 + x_3 \tag{5.11}$$